ISAS - INTERNATIONAL SCHOOL
FOR ADVANCED STUDIES

PROTEIN FOLDING TRANSITION NEAR INTERFACES

Thesis submitted for the Degree:
Magister Philosophiae

Candidate:
Serge Cattarinussi

Supervisor:
Dr. Giancarlo Jug

Academic Year 1988/89

TRIESTE

SISSA - SCUOLA
INTERNAZIONALE
SUPERIORE
DI STUDI AVANZATI
TRIESTE
Strada Costiera 11

– INDEX –

7. Appendix

7.1 Numerical algorithm for enumerating lattice walks.

7.2 SAW and Globule configurations for 2×2 cells.

7.3 SAW configurations for 3×3 cells.

1. INTRODUCTION

1.1 Protein Folding Phenomenology

Proteins are macromolecules composed by chains of *amino acid residues.* Their characteristic molecular mass is around *20.000* which corresponds to *150 - 180* residues.

The ordered sequence of amino acids is called the *primary structure* of the protein. This structure determines the biological function of a protein and the substitution of a single amino acid residue by another can make the protein unefficient from the biochemical point of view.

The chemical bond which links the residues to each other is called the *peptide bond* which exhibits a resonance-stabilized structure:

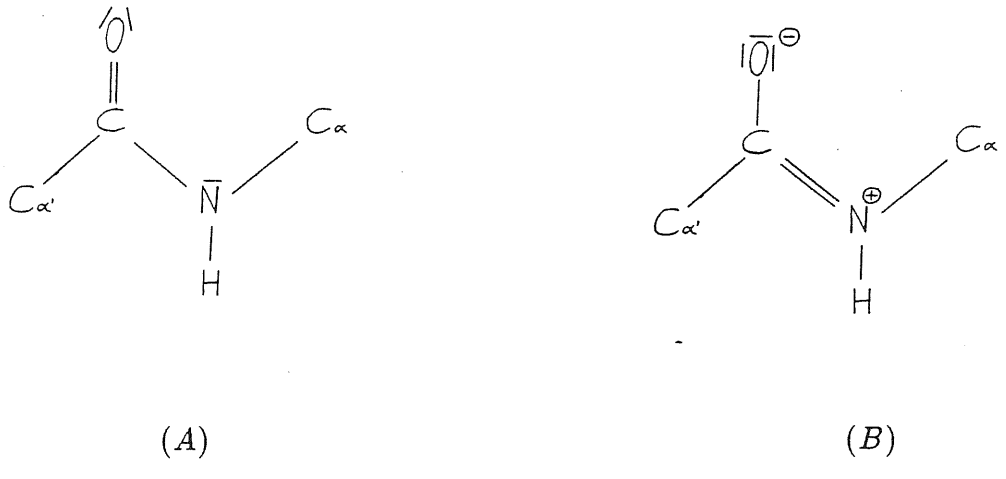

(A) (B)

fig.1

The above two limiting electronic structures of the bond form a hybrid which contains about 60% of (A) and 40% of (B) . The electronic distribution (A) allows free rotation around the bond $C-N$ whereas the distribution (B) restricts rotation. The overall result is that the molecule can only rotate around $N-C_\alpha$ and $C_\alpha - C$ bonds.

The rotation angles φ and ψ around these bonds have a limited range of values because

of steric repulsions between residues. The conformation of a polypeptide chain may be fully described by giving the angles φ and ψ for each peptide bond.

Intramolecular or extramolecular hydrogen bonds between H atoms of $N-H$ groups and O atoms of $C=O$ groups can stabilize some partial chain conformations called $\alpha-helix$, $\pi-helix$, $\beta-sheets$ and so on. Such conformations are called *secondary structure.*

Usually a natural protein is not entirely ordered. Along the chain we can find alternatively ordered (for instance $\alpha-helix$) and non-ordered, highly flexible, segments. This flexibility allows the chain to fold over and to acquire a new spatial structure called *tertiary structure* which determines its biochemical functionality. Because of their spherical overall shape, folded proteins are named *globules.*

Sometimes proteins show a *quaternary structure* which results from the aggregation of polypeptides by specific interactions.[3]

Summarizing, we can say that a protein is a many-level system in which the conformation at a specific level depends on the geometric properties of the previous level, on the interaction forces between its elements and on the interaction with the environment.

As already mentioned, tertiary structure enters in an essential way in the biological function of a protein. But protein globules are stable only under optimal conditions and can be *denaturated* by environmental changes such as a rise in temperature, variation of pH , addition of a variety of denaturant molecules or increase in pressure.

This *folding–unfolding* transition is still not well understood but it appears to be a self-assembly process in that all the information required to obtain a definite globular conformation is present in the amino acid sequence. Under appropriate conditions the process occurs spontaneously, probably also *in vivo* after the biosynthesis of the linear polypeptide chain.[4]

The physical forces which are involved in the protein folding are essentially the so-called "weak forces" such as *Van der Waals* forces, *hydrogen* bonds and first of all *electrostatic* interactions.

Simple considerations about the number of possible conformations of a protein show

that folding is not achieved by simply sampling randomly all possible conformations until the one with the lowest free energy is encountered. Cooperative processes like in well known physical phase transitions can be envisaged.

As the environment is gradually altered towards conditions favourable for protein unfolding, the folded conformation initially changes very little. The protein then becomes fully unfolded within a rather limited range of conditions. This behaviour, as shown in fig.2, is characteristic of phase transitions.

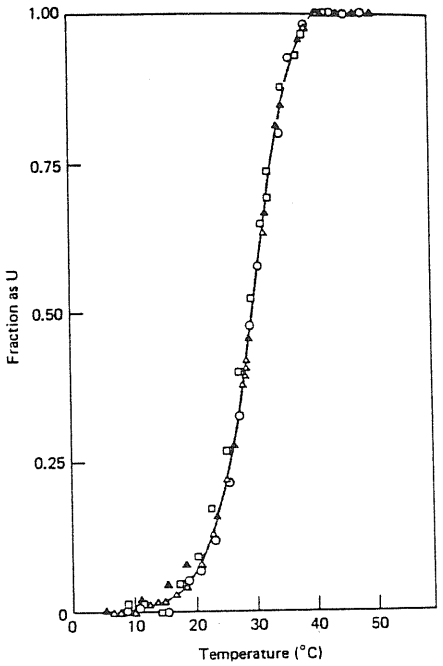

The temperature-induced unfolding of bovine ribonuclease A in HCl-KCl at pH 2.1 and 0.019 ionic strength, measured by the increase in viscosity (□) and the decreases in optical rotation in 365 nm (○) and UV absorbance at 287 nm (△—△). The filled triangles show measurements of a second melting after cooling from 41°C for 16 h, indicating slight irreversibility at low temperatures. (Adapted from A. Ginsburg and W. R. Carroll, Biochemistry 4:2159–2174, 1965.)

fig. 2

The biological functions of proteins almost invariably depend upon their direct, physical interaction with other molecules. Virtually every substance with which a cell comes into contact is recognised and bound by some protein.

Proteins may bound very tightly and specifically to other proteins, generating large complexes; to nucleic acids, especially when controlling their replication and expression;

to polysaccharides,especially important being those on the surface of cell membranes; and to lipids, often becoming incorporated within membranes.

Proteins are generally classified according to purpose and consequences of bindings; for example, structural proteins, enzymes, repressors, immunoglobulins, hormones, receptors, membranes transport proteins and proteins of motility. The interactions between proteins and ligands are specific, that is, there is discrimination between even closely related ligands. Specificity is related to the existence of binding sites, which comprise relatively little of the protein structure, often just a small patch on the surface. Even relatively small, localized alterations of the protein, therefore, can produce large changes in its binding of ligands, without changes in the overall protein conformation.

The fact that different binding sites, on a protein, interact, goes under the name of *allostery* [2] and is closely related to protein flexibility. Two opposing, extreme models have been proposed to explain how the binding of one ligand molecule by a protein can alter the affinity of another site for its ligand, either increasing or decreasing it.

The *Sequential Model*[2] is based on the idea that a protein is sufficiently flexible that binding of a ligand at one site can readily alter directly its conformation at another, thereby affecting its affinity for a ligand.

The *Conserted Model*[2] stipulates the existence of a conformational equilibrium between two alternative conformations of the protein. The binding of a ligand at one site is supposed to alter this equilibrium and, since different conformations have different affinities for ligands, it modifies the global affinity for ligands.

Certainly folding–unfolding transition can be viewed as an extreme case of allostery in which a change in protein–solvent interaction completely alters protein functionality.

Allostery has an essential role in regulating enzymatic activity. An enzyme catalyses chemical reactions within and between its *substrates*, those molecules that bind in the correct orientation at its active sites. It is impossible on the basis of the present evidence to say exactly how an enzyme acts. At best it is possible to rationalize how an enzyme might do so. In short, we will just say that there is a large entropic advantage in a reaction occurring on an enzyme. The greater the number of reactants, the greater the advantage.

For example, the probability of simultaneous encounters between three or four reactants in solution when all are present at normal concentrations is essentially nil, whereas ternary and quaternary complexes on an enzyme could be readily envisaged.

In vivo, enzymes do not normally act independently and in isolation. Instead, their function is just one of the many steps in metabolism, which consists of a maze of converging degradative pathways, on the one hand, by which food and endogenous reserves are converted to energy and a few simple products, and, on the other hand, of a maze of diverging and interlocking biosynthetic pathways by which the degradative products are converted to proteins, nucleic acids, lipids, and so forth. In order for this complex metabolic system to work, each enzyme must have the appropriate catalytic properties.[2]

The catalytic capabilities required for each enzyme will depend upon its metabolic role but they also must respond to changes in metabolism. This control of enzyme catalysis is accomplished by varying both the quantity of enzyme present and its catalitic activity. One of the predominant ways in which enzyme activity is controlled is by allosteric interactions, and perhaps, as an extreme case, by folding–unfolding transitions.

Obviously, the conformational properties of a protein are fundamental whatever its biochemical function. The study of these properties by mean of non–specific models could show a non-trivial behaviour common to a number of processes and therefore serves to obtain a general framework within which a better or simpler understanding of these processes could be obtained.

1.2 Proteins at Membranes : Phenomenology

Membranes participate directly to all the functions of a cell. In particular they provide for *active transport* and for many other important bioenergetic processes. For instance ATP is synthesized in mitochondria membrane. Bioelectrical phenomena also have their origin in the membrane of nerve cells.

Membranes are composite structures which are essentially made up of *proteins*, $20\% - 75\%$, and *lipids*, $80\% - 25\%$. The lipid portion is composed by *phosphoglycerides*

and *sphingomyelins* which are molecules with a polar head and a non polar, hydrophobic, tail. In aqueous solutions these molecules may form micelles, monomolecular or bimolecular layers.[3]

Present theories describe membranes as fluid systems which are composed of bimolecular layers of phospholipids and various globular embedded proteins.

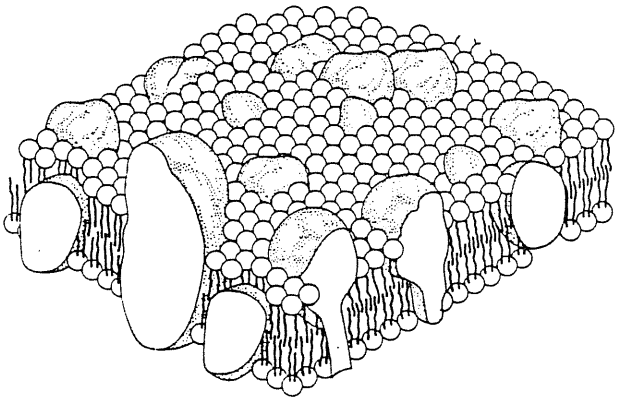

Model of a cell membrane from a protein-phospholipid bilayer

fig.3

The depth to which the proteins penetrate the lipid layer is determined by the amino acid sequence. The membrane proteins are strongly associated to the lipids and this association stabilizes the native conformation of the membrane proteins. Often they can be extracted only in a denaturated form using detergents.

The membrane proteins within the lipid double layer can move freely and are able to diffuse laterally. This characteristic is fundamental for enzymatic functions of some membrane proteins because it allows enzymes or substrates to diffuse toward each other in the membrane.

The variability of the ratio of protein to lipid found in biological membranes, no doubt reflects the variations in the functions of different membranes. Myelin which functions mainly as an insulator is composed only by 18% of proteins. Mitochondria inner membrane is involved with many enzymatic and transport processes. These functions are fulfilled by proteins and we observe that this membrane is composed by 75% of

proteins.

Membrane proteins fall into two broad categories, depending upon how they are bound to the membrane. *Peripheral proteins* are those that can be removed from membranes by relatively mild treatments. These proteins are generally stable in aqueous solutions and contain no tightly bound lipid material. Examples of this kind of proteins are *cytochrome C* from mitochondrial membrane and *spectrin*, a component of erythrocyte membranes. *Integral proteins* are more difficult to remove and tend to aggregate when in an aqueous environment.[5]

Some interesting, still open, questions arise about protein-lipid interactions :

- Does a membrane protein perturb the lipid phase adjacent to it ?
- How much do lipids affect the protein properties ?
- Do lipids penetrate the protein or lie on its surface ?

Without doubts, even a partial answer to these questions will help in the understanding of many features of the countless physiological processes that involve proteins and membranes.

In chapter 3, we are going to tackle the second of the above questions. We will use a, perhaps oversimplified but interesting, model for the adsorption of a protein on an attractive surface. From the biophysical point of view, the most interesting result is the discovery of the existence of a coupling between the coil–globule and the adsorption–desorption transitions. This result is obtained with the simple assumption that the attractive force between the surface and the protein is homogeneously distributed along the membrane surface. The important feature is the "geometrical" and non specific nature of the coupling.

On the one hand, omissions apart, it appears that the direct effect, on a protein, of the adsorption has not been fully taken into account in the description of any biological process. On the other hand, we know that, often, proteins are not synthesized in their final form [14] and that, before becoming functional, they undergo a number of transformations induced by the enzymatic activity. We can then imagine that such transformations of a protein are strongly influenced by its conformational state. Thus, a protein which would swell when in contact with a cell membrane, would allow for the action of the membrane

bound enzymes. Conversely, a protein which would be in a swollen conformation in the cytoplasma, could, after having undergone some enzymatic transformations, collapse and become functional when in contact with a membrane.

In a slightly different context, it has been proved that the membrane can have some influence on embedded proteins. A modification of physicochemical membrane properties such that a variation of its chemical composition or an order-disorder transition in its double layer structure have been observed to induce modifications of the activity of membrane bound enzymes [15].

Since lipids are smaller molecules which are much easier to study than proteins, much more is known about the inverse problem, that is, the influence of proteins on membranes. Particular attention has been payed to the modification of membrane fluidity by embedded proteins. Jahnig [16] has pointed out that a possible explanation for the high diffusion rate of proteins in gel–state bilayers, could be that the immediate environment of the protein in the gel is disordered and fluidlike so that the protein melts its way through the gel in a manner recalling the passage of a wire through a block of ice.

The membrane fluidity properties are relevant for a number of biological processes such as, for instance, endocytosis, which requires condensation of ligand–receptor complexes [14], or chemoreception, which, in some cases, requires diffusion of receptors and adsorbed ligands toward each other [17].

About the effects of proteins on bidimensional films, it is worth recalling the work by Graham and Phillips [21]. The authors are concerned with foamability of protein aqueous solutions and with the stability of formed foams. As shown in figure 4, the foams considered are made up of small irregular polygonal air cells divided by a water film with embedded globular or coil proteins.

The relevant result is that the foams stabilized by proteins which are in the native, globular, state are more stable than foams prepared with unfolded, denaturated, proteins.

This seems to be a good example of the importance of the conformation of proteins in their interaction with a surface.

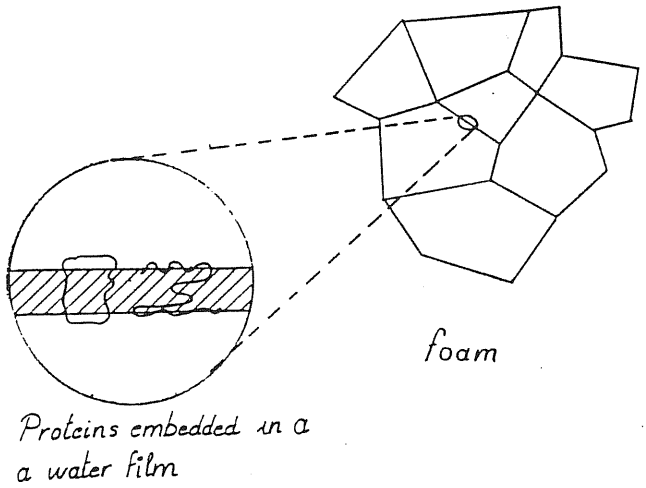

fig. 4

1.3 Random Walk Models for Protein Folding

From the point of view of statistical physics, proteins are long flexible chains which undergo a folding phase transition due to the interplay of weak chemical forces between its elements (the amino acid residues) and the solvent molecules.

As already stated, these weak chemical forces are essentially Van der Waals interactions, hydrogen bonds and a set of dipolar electric interactions which go under the name of hydrophobic effects.

Details of such numerous and vastly complex interactions are fundamental for the determination of the final state of a globular protein. Being this final state so important for the biological functionality of a specific protein, we should attempt to predict it from the only information source that is available on the protein : the amino acid sequence or primary structure.

Unfortunately this seems to be very difficult or even impossible to achieve owing to the probable relevance of kinetic effects and to the incommensurable number of possible configurations which makes numerical simulations almost hopeless.

However, the prediction of the final globular state is certainly beyond not only the possibilities but also the aims of physics, which is actually concerned with the description of as general and universal features as possible of a system.

There are two procedures by which physics can achieve generality and universality. The first – and deeper – consists of elucidating the nature of interactions in a class of systems in order to elaborate a theory, whereas the second consists of modelling a system in such a way that only a given aspect of the system's behaviour is outlined. Hence, systems can be shown to exhibit the same characteristics even if they are quite different.

From now on, we adopt the second point of view in order to obtain a sufficiently general and universal description of the protein behaviour near a surface. Obviously the risk is to oversimplify the system under consideration (protein) and thus to construct a model that shows only trivial properties. Nevertheless our first, drastic step in modelling proteins will be to ignore the distribution of hydrophobic and hydrophilic residues along the chain, therefore considering it as a polymer with homogeneous global interactions between "protein" (polymer) residues and solvent molecules.

Such a drastic simplification should be considered as a *first step* towards more realistic models in which a *random* distribution of hydrophilic and hydrophobic residues will be taken into account.

The Flory-Huggins Model.[1]

The *mean field approach* within the Flory-Huggins model is based on a representation of the polymer chain as a random walk on a lattice :

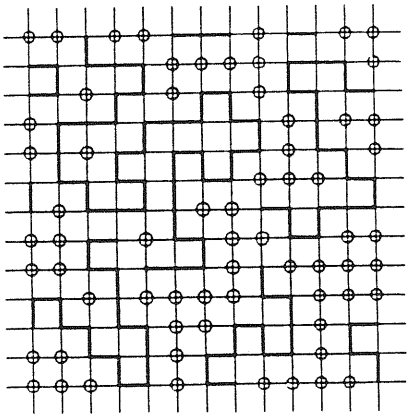

fig.5

where each lattice site is either occupied by one and only one monomer or by a solvent molecule. The fraction of sites occupied by monomers is denoted by ϕ , which is related to the monomer concentration c through $\phi = ca^d$ with a the lattice constant and d the dimensionality of "space".

Defining the mixing free energy per site as the difference between the effective free energy and the sum of the weighted free energy for pure solvent and pure polymer, we have the the usual thermodynamic relation :

$$\left(\frac{F_{mix}}{T}\right)_{site} = -\left(S_{mix}\right)_{site} + \left(\frac{E_{mix}}{T}\right)_{site} \qquad (1)$$

Using the following expressions

$$-(S_{mix})_{site} = \frac{\phi}{N}\ln\phi + (1-\phi)\ln(1-\phi) \tag{2}$$

and

$$\left(\frac{E_{mix}}{T}\right)_{site} = \chi(1-\phi)\phi \tag{3}$$

we find

$$\left(\frac{F_{mix}}{T}\right)_{site} = \frac{\phi}{N}\ln\phi + (1-\phi)\ln(1-\phi) + \chi(1-\phi)\phi \tag{4}$$

Expanding the regular terms for small ϕ in the above equation we find

$$\left(\frac{F_{mix}}{T}\right)_{site} = \frac{\phi}{N}\ln\phi + \frac{1}{2}\phi^2(1-2\chi) + \frac{1}{6}\phi^3 + \ \ldots \tag{5}$$

where χ is the temperature dependent *Flory interaction parameter* and N is the number of monomers in the chain.

It is possible to discuss the existence of a phase transition (or phase separation) on the free energy equation (5). The essential property is the curvature of $F(\phi)$. Roughly speaking we can say that if $F(\phi)$ is convex everywhere, there is no phase separation and the monomer concentration ϕ is uniformly distributed. This situation corresponds to swollen polymer chains in the solvent.

If $F(\phi)$ is concave in a domain of ϕ values then it will be advantageous for the system to separate into two phases characterized by a low and a high monomer concentration ϕ' and ϕ'' .

The high monomer concentration phase can be interpreted as a collapsed chain region whilst the low monomer concentration phase corresponds to the almost pure solvent.

From equation (5) we can draw the following plot :

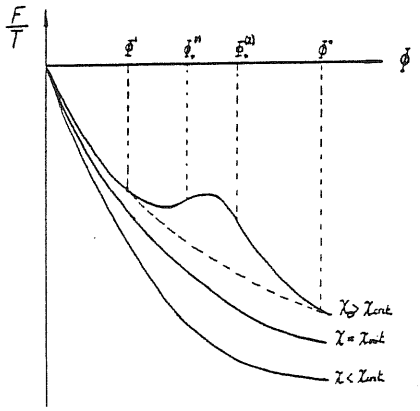

fig.6

and we see that, for $\chi > \chi_{crit}$, $F(\phi)$ effectively presents a concave region. χ being temperature dependent, we conclude that below a critical temperature Θ such that $\chi(\Theta) = \chi_{crit}$ the macromolecule will tend to collapse. The following equation

$$\frac{\partial^2}{\partial \phi^2}\left(\frac{F}{T}\right) = \frac{1}{N\phi} + \frac{1}{1-\phi} - 2\chi = 0 \tag{6}$$

gives the values of ϕ at the inflexion points of $F(\phi)/T$. It defines also a function

$$\chi(\phi) = \frac{1}{2}\left(\frac{1}{N\phi} + \frac{1}{1-\phi}\right) \tag{7}$$

which is plotted in fig.7

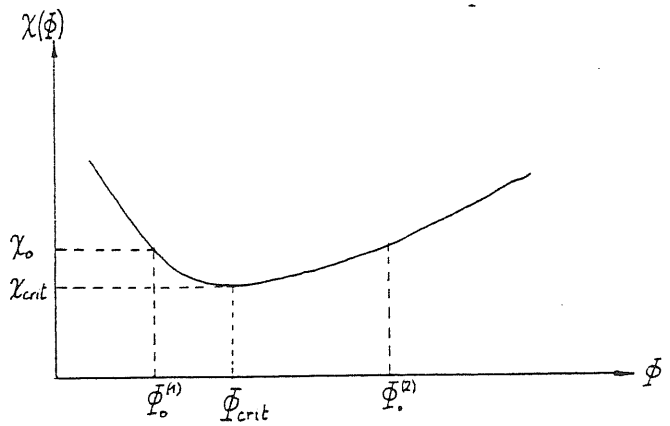

fig.7

$\phi_0^{(1)}$ and $\phi_0^{(2)}$ correspond to the inflexion points of $F(\phi)/T$ with the Flory interaction parameter $\chi = \chi_0 > \chi_{crit}$. From fig.6 we see that in order to find the value of χ_{crit} and ϕ_{crit} we just have to require that $F(\phi)/T$ has no more inflexion points.

From fig.7 we then note that this requirement is equivalent to ask $\chi(\phi)$ to be a minimum. Therefore, from the condition

$$\frac{\partial \chi}{\partial \phi} = 0 \tag{8}$$

we easily find

$$\phi_{crit} = \frac{1}{N^{1/2}+1} \longrightarrow 0, \qquad N \longrightarrow \infty \tag{9}$$

$$\chi_{crit} = \frac{(1+N^{1/2})^2}{2N} \approx \frac{1}{2} + N^{-1/2} \longrightarrow \frac{1}{2}, \quad N \longrightarrow \infty \tag{10}$$

Following Edwards[18], we can write a slightly more general free energy density function for polymer in a good solvent (virial expansion) :

$$\left(\frac{f}{T}\right) = \frac{c}{N}\ln c + \frac{1}{2}vc^2 + \frac{1}{6}w^2c^3 + \ \ldots \tag{11}$$

which is independent of any lattice model. Using the definition $\phi = ca^3$ we have a correspondence between equations (5) and (11) only if we define

$$v = a^3(1-2\chi) \propto T - T_\Theta + O[(T - T_\Theta^2)] \tag{12}$$

where v is called the *Flory excluded volume parameter.*

Summarizing we will say that for $\chi > 1/2$ and therefore $v < 0$ attractive forces are predominant and the polymer chain will be in a collapsed state, referred to as the Globule. Conversely for $\chi < 1/2$ i.e. $v > 0$, the steric repulsion and entropic effects dominate

and the chain will tend to swell (Coil state). For $\chi = 1/2$ i.e. $v = 0$ we have the so-called *coil-globule transition* which happens at a particular temperature Θ such that $\chi(\Theta) = 1/2$.

Ideal and real chains.

Having seen how we can describe, in a mean field picture, the folding of a polymer chain, we return now to random walk lattice models with the intent to have a more geometrical insight.

Ideal chains. The simplest idealization of a flexible polymer chain consists of replacing it by a *simple* random walk on a periodic lattice. At each step, the next jump may proceed towards any of the nearest-neighbour sites and the statistical weight for all these possibilities is the same.

With such an idealization, chain properties are easily visualized. For instance the entropy of a chain starting at the origin $\mathbf{r} = \mathbf{0}$ and ending at a lattice point $\mathbf{r}$ is

$$S(\mathbf{r}) = \ln [N_N(\mathbf{r})] \tag{13}$$

with $N_N(\mathbf{r})$ the number of walks starting at $\mathbf{r} = \mathbf{0}$ and ending at $\mathbf{r}$. It is quite obvious that the total number of random walks with N steps is given by :

$$N_N(tot) = \sum_{\mathbf{r}} N_N(\mathbf{r}) = z^N \tag{14}$$

where z is the lattice coordination number. For instance $z = 4$ in a two dimensional square lattice. Denoting by $\mathbf{a}_n$ the $n - th$ step in a random walk, we have

$$\mathbf{r} = \sum_n \mathbf{a}_n$$

and because of the statistical independence of the $\mathbf{a}_n$'s

$$\langle \mathbf{r}^2 \rangle = \sum_{m\ n} \langle \mathbf{a}_n \mathbf{a}_m \rangle = \sum_n \langle \mathbf{a}_n^2 \rangle = Na^2 \tag{15}$$

So an ideal chain will have a characteristic size

$$R_0 = \left(\langle \mathbf{r}^2 \rangle \right)^{1/2} = aN^{\nu} \tag{16}$$

with the characteristic exponent $\nu = 1/2$.

Real chains. A slightly more realistic description of a polymer chain in a solvent can be achieved by considering a self-avoiding walk (SAW) on a lattice. In this way we take into account steric repulsions because two monomers cannot occupy the same site.

Two main methods have been employed to investigate the complex geometrical properties of SAWs :

(i) Numerical methods, which include exact enumeration of walks for finite N and Monte-Carlo algorithms.

(ii) Renormalisation group methods which are the subject of the next sections.

Here we just present some essential results.

The total number of SAWs of N steps, which is related to the entropy of chains, has the asymptotic form

$$N_N(tot) \sim Z^N N^{\gamma - 1} \tag{17}$$

Z, which is reminiscent of z in equation (14), is the effective lattice connectivity, that is the effective number of possible choices at each step, for $N \longrightarrow \infty$, on an infinite lattice. Obviously Z depends on the lattice and $Z < z$. On the contrary, γ is a universal exponent which depends only on the dimensionality d of the system. For $d = 2$, $\gamma \cong 4/3$.

The characteristic size or mean end-to-end distance is asymptotically given by

$$R = \left(\langle \mathbf{r}^2 \rangle\right)^{1/2} \sim aN^{\nu} \tag{18}$$

with the universal exponent $\nu \cong 3/4$ and $3/5$ in dimension $d = 2$ and $d = 3$, respectively.

Before ending this section we consider again equation (5) in which we set $\chi = 1/2$. We note then that at the coil-globule transition the ϕ^2 term disappears. This means that the two body interactions vanish by cancellation of repulsive and attractive effects. Apart from residual three-body interactions, the chain at Θ-point will have an ideal behaviour. In particular we expect, for $d = 2$:

$$\nu_{\Theta} \approx 1/2 \tag{19}$$

1.4 Random Walk Models for Polymer Adsorption

In the presence of an attractive surface a polymer chain should be adsorbed, but in this case it will acquire an essentially two-dimensional (or one-dimensional if we are in a two-dimensional space) configuration with very low entropy.

In actual fact, there are two competing effects that determine the state of the polymer chain. The minimum energy tendency favours the adsorbed phase whereas the maximum entropy tendency favours the "free" states. A phase transition, with temperature as the driving parameter, will occur. Above a special temperature T_a the chain will be free (three dimensional), below T_a it will be adsorbed.

The fundamental observation is that for $T < T_a$ we have the formation of an adsorbed layer of polymer with a characteristic thickness D proportional to the polymerisation index N when we consider a polymer solution, and independent of N for an adsorbed single chain. The reason is that when *many chain are adsorbed*, the monomer-monomer repulsions compensate the surface attraction.

For $T > T_a$ one can observe the formation of a *depletion layer* with decreasing monomer density $\varphi(Z)$ near the surface $Z \longrightarrow 0$. (See fig.8).

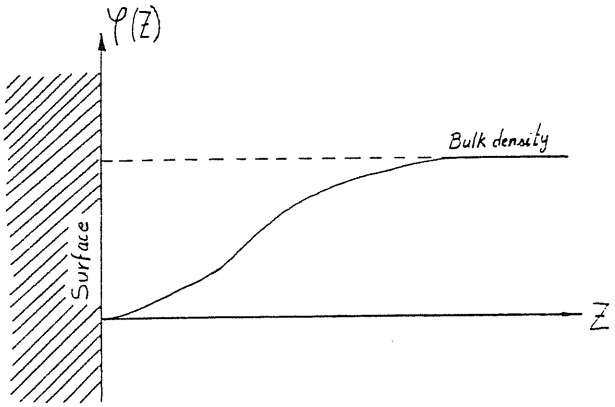

fig.8

We are going to briefly describe two different scaling approaches to this problem. The first is the simplest and will be presented with some details while for the second only the main ideas and results will be given.

Scaling relations have been first introduced as an ad-hoc way of adapting the classical Landau theory (mean-field) in order to reproduce the correct behaviour of magnetic systems near the critical point.

Here we are mainly concerned with what we call finite-size scaling, which has the basical assumption that, in the vicinity of the critical temperature, the behaviour of a system is determined by the scaled variable

$$y = \frac{L}{\xi(T)} \tag{20}$$

where L is the finite linear size of the system, and $\xi(T)$ the bulk correlation length.

Using this finite-size scaling hypothesis, we can derive the following form for the free energy (or chemical potential) of a confined self–avoiding chain:

$$\mu = \mu_0 + N\left(\frac{a}{D}\right)^{5/3} - \delta\frac{aN}{D} \tag{21}$$

where μ_0 is the chemical potential for a free chain and the third term states that, of the N monomers, only a fraction a/D is in the first layer and benefits from the effective attraction δ. The second term represents the confinement energy $\mu_{conf.}$, in a layer $D < R_0$, with R_0 the characteristic size of the chain.It can be derived as follow.

According to our scaling hypothesis, $\mu_{conf.}$ must be a function of R_F/D, where R_F, which is the mean square root of the end-to-end distance of the chain, is equivalent to ξ, and D is equivalent to L.

Furthermore, $\mu_{conf.}$ must be a linear function of N, as it should be clear from the following figure:

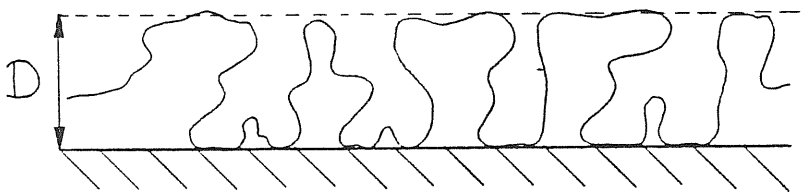

fig.9

Since doubling N simply doubles the number of "loops", retained near the surface.

Thus, with φ a regular function

$$\mu_{conf.} \approx \varphi\left(\frac{R_F}{D}\right) = \varphi\left(\frac{aN^{3/5}}{D}\right) \tag{22}$$

and

$$\mu_{conf.} \sim N \tag{23}$$

So asymptotically, for $N \longrightarrow \infty$, we must have:

$$\mu_{conf} \approx \left(\frac{aN^{3/5}}{D}\right)^{5/3} = N\left(\frac{a}{D}\right)^{5/3} \tag{24}$$

Minimizing equation (21) with respect to D we obtain:

$$D_{single\ chain} \approx a\delta^{-3/2} \tag{25}$$

Even if very precise experimental and Monte-Carlo determination of D are still missing, it seems that the above scaling analysis is more reliable than simple mean field theory.

Another much more involved scaling analysis of adsorption of polymer chains at surfaces was performed by Eisenriegler, Kremer, and Binder in reference [9].

This scaling analysis is based on the following ideas:

There exists a strong formal analogy between the n-components spin vector model of a magnet, and polymer configurations models. Such an analogy was first pointed out by De Gennes (for a review, see reference [1]), who established the equivalence between the Curie-point of the ferromagnetic-paramagnetic transition and the asymptotic behaviour of a polymer chain. The physical reason for this analogy lies in the fact that the relevant spin-spin correlation paths near the Curie critical point are self-avoiding walks on the lattice of spins. When $t = T - T_c \longrightarrow 0$, spin-spin correlations diverge, and this corresponds, for the polymer model, to infinite SAWs ($N \longrightarrow \infty$).

Magnetic systems have been extensively studied also in the presence of a surface. The behaviour of such systems is summarized by the following phase diagram:

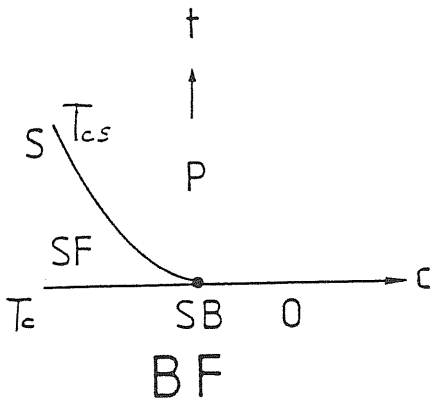

fig.10

where t is the temperature and c a variable which can be related to a "surface energy" [9].

For $c \geq 0$ we have an order-disorder (ferromagnetic-paramagnetic) transition, which occurs simultaneously in the bulk and at the surface at a temperature T_c.

For $c < 0$ the surface orders at a temperature $T_{cs} > T_c$, so in a region characterized by $c < 0$, and $T_c < T < T_{cs}$, we have a ferromagnetic surface (SF), and a paramagnetic bulk (P).

Like for the Θ-point transition, the equivalence with the polymer chain adsorption is established by noting that the adsorbed phase of the polymer chain corresponds to a situation where the surface of the corresponding magnet orders before the bulk, and the adsorption-desorption temperature T_a corresponds to the multicritical point SB of simultaneously ordered bulk and surface.

Translating the results for the semi-infinite system's magnetic correlation functions to the polymer problem yields many interesting results . We will reproduce here some of these which are relevant for our following analysis.

The presence of a surface breaks the translation symmetry in the direction perpendicular to the surface, and requires therefore the introduction of two characteristic polymer lengths:

$$\langle R^2 \rangle_{\perp}^{1/2}$$

and

$$\langle R^2 \rangle_{\parallel}^{1/2}$$

which are the chain end-to-end mean square root distance in the perpendicular and the parallel directions, with respect to the surface, respectively.

The following scaling relation is found to hold:

$$\langle R^2 \rangle_{\perp}^{1/2} = L^{\nu} \phi_{\perp}(cL^{\varphi}) \tag{26}$$

with $L = Na^2$, $c = 1 - (T/T_a)$, and φ the so called cross-over exponent which governs the "bulk to surface transition".

From the magnetic systems we know that the spin correlation length perpendicular to the surface remains finite when approaching the line S, ($T - T_{cs} = t \longrightarrow 0$; $c < 0$), though it diverges like $t^{-\nu}$ on approaching either SB or O, ($T - T_c = t \longrightarrow 0$; $c \geq 0$), see fig. 10.

Given that $t \longrightarrow 0$ corresponds to $N \longrightarrow \infty$, and consequently $L \longrightarrow \infty$, we have the following analogies and limits:

a) For $c < 0$ (attractive surface), $\langle R^2 \rangle_{\perp}^{1/2}$ must remain finite when $L \longrightarrow \infty$, thus

$$L^{\nu} \propto \phi_{\perp}(cL^{\varphi}) \sim (cL^{\varphi})^{x} \tag{27}$$

So $x = -\nu_B/\varphi$, and

$$\langle R^2 \rangle_{\perp}^{1/2} \sim \mid c \mid^{-\nu/\varphi} \sim (T - T_a)^{-\nu/\varphi} \tag{28}$$

b) For $c = 0$ (neutral surface), and $c \geq 0$ (repelling surface), we have:

$$\langle R^2 \rangle_{\perp}^{1/2} \sim L^{\nu} \sim N^{\nu} \tag{29}$$

which corresponds to the usual bulk behaviour.

At this point we must recall that scaling analysis cannot give us the value of critical exponents. These must be calculated either analytically by evaluation of the partition function, or by numerical methods (Monte-Carlo or exact configuration enumeration for finite systems plus extrapolation methods). Eisenriegler et al. have performed an exact analytic evaluation of critical exponents for the adsorption-desorption transition of ideal chains, and a Monte-Carlo analysis of real chains.

Before presenting their results, we must emphasize that the study of ideal chains is not only an academic exercise. As already stated, polymer chains at the Flory Θ-point are fairly well described by ideal chains, apart from residual three body interactions that don't cancel in the mean field expression for the free energy.

The study of ideal chain adsorption is then doubly interesting: On the one side it allows for the description of real chain adsorption at the Flory temperature. On the other side, if by a different method we can show that real chain adsorption at Θ-point deviate from ideal chain behaviour, then we will have proved the relevance of high order terms in the free energy expression.

Ideal chains.

For the ideal, non-interacting, chains the exponents involved in a scaling description are the bulk correlation length exponent, or size exponent, $\nu = 1/2$, and the cross-over exponent $\varphi = 1/2$, which have been found exactly [9]. Defining $\nu_s = \nu/\varphi = 1$, we have (see equation(28)and(29)):

$$\langle R^2 \rangle_{\perp}^{1/2} \sim \mid T - T_a \mid^{-\nu_s}, \qquad \text{for } c < 0 \text{ (attractive surface)}$$

$$\langle R^2 \rangle_{\perp}^{1/2} \sim N^{\nu}, \qquad \text{for } c \geq 0 \text{ (repulsive or neutral surface)}$$

In the last case, we find again the well known behaviour of ideal (simple random walk) chains in the bulk. Another coefficient of interest is the entropic exponent γ, which governs the growth of the number of configurations Z_N, when $N \longrightarrow \infty$ and the starting point is fixed on the surface. It is found:

$$\gamma = \tfrac{1}{2} \ , \qquad \text{for attractive surface } (\ c < 0 \ )$$

$$\gamma = 1 \ , \qquad \text{for repulsive or neutral surface } (\ c \geq 0 \ )$$

Real chains.

For chains with excluded volume interaction, Eisenriegler et al. find, through Monte-Carlo analysis, the following values:

$$\begin{aligned} &\nu_{(3d)} \cong 0.59 && c \geq 0 \\ &\nu_{(2d)} \cong 0.75 && c \geq 0 \\ &\nu_{s(3d)} \cong 1 && c < 0 \\ &\nu_{s(2d)} \cong 1.31 && c < 0 \end{aligned}$$

which leads to a cross-over exponent

$$\varphi = \left(\frac{\nu_{(3d)}}{\nu_{s(3d)}} \right) \cong 0.59 \tag{30}$$

$$\varphi = \left(\frac{\nu_{(2d)}}{\nu_{s(2d)}} \right) \cong 0.57 \tag{31}$$

2. REAL-SPACE RENORMALISATION METHODS FOR RANDOM WALK MODEL

2.1 Position space renormalisation group

We have already presented in the introduction (sections 1.3 and 1.4) a mean field and a scaling approach to the statistical properties of polymers. It is obvious that the polymer problem is just an interesting but very small application area of these two theoretical approach. Indeed every time we deal with a system presenting a second order phase transition, the same theoretical approach can be employed.

The mean field approach fails in describing correctly the behaviour of generalized specific heats and susceptibilities as well as coexistence curves near the critical point. Asymptotically, these physical quantities are found to follow some "mysterious" power laws, whose exponents are related to each others by some equally "mysterious" scaling relations. We know that the weakness of the mean field approach consists of neglecting the fluctuations, and therefore the very large correlations that arise near critical points. Scaling relations exist because, due to large fluctuations, the behaviour of physical quantities near criticality reflects only the properties of the system, whose characteristic length is the fluctuation size range.

This leads to another fascinating characteristic of critical phenomena which is called *universality* and expresses the fact that several apparently unconnected systems, such as, for instance, polymer chains and magnets, have common critical properties. The only available approach which describes all of the above features is the so-called Renormalisation Group Theory.

The task of this theory is to explain the origin of the power law behaviour singularities of universality and of scaling relations, as well as providing ways of calculating exponents and other universal properties.

With notations normally used for magnetic systems, we will now present some formal and very general aspects of real space renormalisation.

Let the general Hamiltonian be $H(\vec{\mu}, \{s_i\})$, with $\vec{\mu} = (K_1,\ K_2,\ \ldots)$ a vector in the

parameter space, and $\{s_i\}$ the set of statistical variables, for instance the spin variables in an Ising spin lattice model.

$\vec{\mu}$ represents all the parameters we need to describe the many body interactions between the statistical variables $\{s_i\}$.

The partition function is the following sum over the spin configurations:

$$Z_1 = \sum_{\{s_i\}} e^{-\beta H(\vec{\mu},\{s_i\})} \tag{32}$$

By formal *coarse graining*, this sum can be carried out in two steps:

$$Z_1 = \sum_{\{s'_p\}} \sum_{\{s_i\}|\{s'_p\}} e^{-\beta H(\vec{\mu},\{s_i\})} \tag{33}$$

where $\{s_i\}|\{s'_p\}$ denotes all the configurations $\{s_i\}$,which are compatible with a special fixed configuration $\{s'_p\}$, where $\{s'_p\}$ are some rescaled variables.

To be more explicit, we can consider the special case of a two dimensional spin lattice in figure 11.

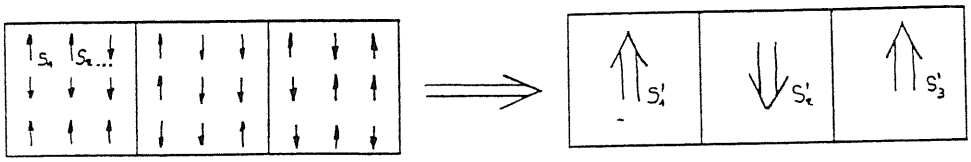

fig.11

If we now want to describe a system near T_c , where the microscopic structures (i.e. the detailed configurations $\{s_i\}$) are irrelevant, then we can just calculate the partition function by summing over the configuration $\{s'_p\}$ introducing a new set of parameters $\vec{\mu}'$, which represents the interactions of the "coarse grained" statistical variables, and therefore a new Hamiltonian with new partition function :

$$Z_2 = \sum_{\{s'_p\}} e^{-\beta H'(\vec{\mu}',\{s'_p\})} \tag{34}$$

If details of the microscopic structure are irrelevant, then we must have :

$$Z_1 = Z_2 \tag{35}$$

and we can define :

$$e^{-\beta H'(\vec{\mu}',\{s'_p\})} = \sum_{\{s_i\}|\{s'_p\}} e^{-\beta H(\vec{\mu},\{s_i\})} \tag{36}$$

At this point, we must determine, on the basis of physical arguments and of our calculational possibilities, the function H' and the variables $\{s'_p\}$.

For instance, with spin models, a simple but convenient choice may be $H \equiv H'$ and $s'_p = 1$ if the majority of the spins s_i in the cell p are equal to 1, and $s'_p = 0$ otherwise (majority rule).

It is crucial to notice that, when H' and s'_p are determined equation (36) gives a relation between $\vec{\mu}$ and $\vec{\mu}'$, that we write:

$$\vec{\mu}' = R_b(\vec{\mu}) \tag{37}$$

This transformation in the parameter space is the *renormalisation group transformation*, which is further analysed as follows.

First of all, we assume the existence of a fixed point $\vec{\mu}^*$ such that:

$$\vec{\mu}^* = R_b(\vec{\mu}^*) \tag{38}$$

Then we linearise the transformation near this fixed point $\vec{\mu}^*$ by:

$$\vec{\mu}' = \vec{\mu}^* + J_{R_b}(\vec{\mu}^*)(\vec{\mu} - \vec{\mu}^*) \tag{39}$$

where $J_{R_b}(\vec{\mu}^*)$ is the jacobian matrix evaluated at $\vec{\mu}^*$.

If we first scale our system by a factor b , and then by a factor b' , the global scaling factor will be $b \cdot b'$.

Therefore the following equality (semi-group propriety) must hold:

$$R_b \circ R_{b'} = R_{b \cdot b'} \tag{40}$$

It is also obvious that R_b and $R_{b'}$ must commute:

$$[R_b, R_{b'}] = 0 \tag{41}$$

Thus near $\vec{\mu}^* = (K_1^*, K_2^*, \ldots)$:

$$[J_{R_b}(\vec{\mu}^*), J_{R_{b'}}(\vec{\mu}^*)] = 0 \tag{42}$$

The last equation ensures us that $J_{R_b}(\vec{\mu}^*)$ and $J_{R_{b'}}(\vec{\mu}^*)$ have a common set of eigenvectors $\{\mathbf{e}_i\}$:

$$J_{R_b}(\vec{\mu}^*)\mathbf{e}_i = \lambda_i(b)\mathbf{e}_i \tag{43}$$

$$J_{R_{b'}}(\vec{\mu}^*)\mathbf{e}_i = \lambda_i(b')\mathbf{e}_i \tag{44}$$

Thus:

$$J_{R_{b'}} J_{R_b}\mathbf{e}_i = \lambda_i(b) \cdot J_{R_{b'}}\mathbf{e}_i = \lambda_i(b) \cdot \lambda_i(b') \cdot \mathbf{e}_i \tag{45}$$

But:

$$J_{R_{b'}} J_{R_b}\mathbf{e}_i = J_{R_{b \cdot b'}}\mathbf{e}_i = \lambda_i(b \cdot b') \cdot \mathbf{e}_i \tag{46}$$

Finally:

$$\lambda_i(b) \cdot \lambda_i(b') = \lambda_i(b \cdot b') \tag{47}$$

The equation (47) is satisfied only if:

$$\lambda_i(b) = b^{y_i} \qquad or: \qquad y_i = \left(\frac{\ln \lambda_i}{\ln b}\right)$$

This is a fundamental result, because the y_i 's are nothing else but the already mentioned critical exponents.

The fixed point $\vec{\mu}^* = (K_1^*, K_2^*, \ldots)$ corresponds to the values of the interaction parameters in the Hamiltonian, for which a scaling does not affect the characteristics of the system any longer. This means that the characteristic lengths of the system, and in particular the correlation length, tend to infinity. From the above, we can see that there is a correspondence between a non-trivial fixed point of a renormalisation group transformation and a critical point.

2.2 Cell-Cell Renormalisation for Self-Avoiding Walk Models

We already know that self-avoiding walks on a lattice can be a good idealisation for polymer chains with monomer-monomer steric repulsions. We also know that De Gennes [13] has pointed out that there is a link between chains and magnets, in the limits $N \longrightarrow \infty$ and $T \longrightarrow T_c$ respectively. A renormalisation group theory exists for magnets that allows us to calculate critical exponents near T_c , but we have not yet presented a method for calculating the geometrical properties of SAW's in the limit $N \longrightarrow \infty$.

To do this, we need a kind of partition function for lattice walks, which can be written:

$$Z_{SAW}^{B}(k_B) = \sum_{N=1}^{\infty} C_N \cdot k_B^N \tag{48}$$

where C_N is the number of SAW configurations with N steps, and k_B is the weight associated with each step, also called *step fugacity*.

To introduce this partition function in a less arbitrary way, we can start from the standard Grand Canonical partition function for a system with a variable number of particles:

$$Z = \sum_{\alpha,N} \mathrm{e}^{-\beta[E_\alpha(N)-\mu N]} = \sum_N z_N \cdot k_B^N \tag{49}$$

with:

$$\begin{aligned} k_B &= \mathrm{e}^{\beta\mu} \\ z_N &= \textstyle\sum_\alpha \mathrm{e}^{-\beta E_\alpha(N)} \end{aligned}$$

where N can be associated with the number of steps, and α denotes the different SAW configurations. Therefore $E_\alpha(N)$ is the energy of an N-step SAW in the configuration α, and z_N the usual canonical partition function for an N-particle (step) system.

If we now make the plausible assumption that each configuration has the same energy $E_\alpha = E, \quad \forall\alpha$, then:

$$z_N = \sum_\alpha \mathrm{e}^{-\beta E_\alpha(N)} = C_N \cdot \mathrm{e}^{\beta E} \tag{50}$$

At a given temperature, $\mathrm{e}^{\beta E}$ is a constant, C_N is just the number of N-step SAW configurations, and equation(48) follows.

About the assumption $E_\alpha = E, \quad \forall\alpha$, we emphasize the fact that steric monomer-monomer repulsions are already taken into account in considering only SAW configurations.

To implement the scheme of renormalisation presented in section 2.1, the only transformation we must do is to consider a rescaled lattice, for instance like in figure 12a) and 12b):

a) b)

fig.12

with, for each step on this lattice, a rescaled fugacity k'_B instead of k_B . Then by equating the two partition functions:

$$\sum_{N=1}^{\infty} C'_N \cdot k_B'^N = \sum_{N=1}^{\infty} C_N \cdot k_B^N \tag{51}$$

we obtain, at least implicitly, the renormalisation transformation:

$$k'_B = R_b(k_B) \tag{52}$$

with k_B^* as the fixed point.

As shown in the previous section, we can then calculate the exponent

$$y_1 = \frac{\ln \lambda}{\ln b} \tag{53}$$

which governs the correlation length, or in a polymer theory language, the mean square radius of the chain (a measure of its size) :

$$\langle R^2 \rangle^{1/2} \sim N^{\nu}, \qquad \text{where} \qquad \nu = \frac{1}{y_1}$$

Obviously this is practically unfeasible because of the difficulties that one encounters in determining C_N for $N \longrightarrow \infty$.

We must then carry out an approximation which consists of considering finite lattices or cells[6]. The approximation introduced is uncontrolled but the results can often be surprisingly good. For instance, using the very simple renormalisation scheme shown in figure 13, de Queiroz and Chaves [19] have found $\nu \cong 0.715$, while the expected value is $\nu = 0.75$.

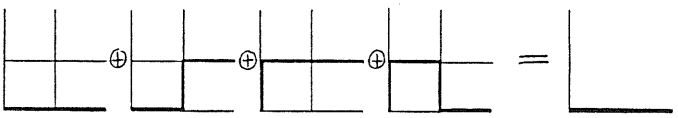

fig.13

The renormalisation transformation corresponding to the figure 13 is:

$$k'_B = k_B^4 + 2k_B^3 + k_B^2$$

$$k_B^* \cong 0.466$$

$$\nu_B = \frac{lnb}{\ln \lambda} \cong 0.715$$

We have just seen how renormalisation group theory can describe the asymptotic properties of SAWs with $N \longrightarrow \infty$ (very long chains). The question we must ask concerns the Θ-point: how can we set up a renormalisation transformation in order to calculate ν_Θ ?

Seno and Stella [11] have introduced a real space renormalisation method

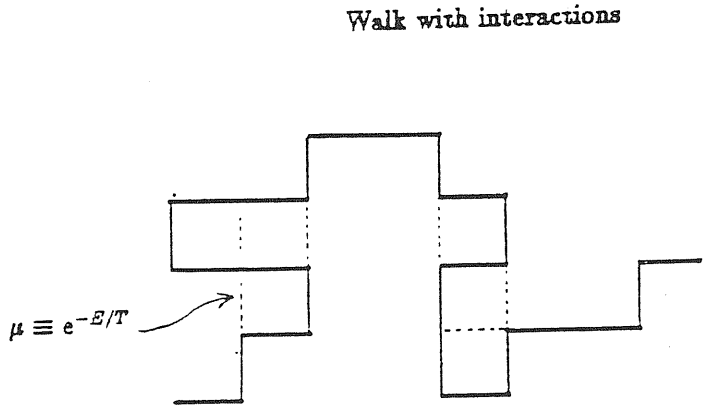

fig 14

based on nearest-neighbour interacting SAWs with $\mu = e^{-\beta E}$, (see figure 14).

They obtained a flow diagram like in figure 15:

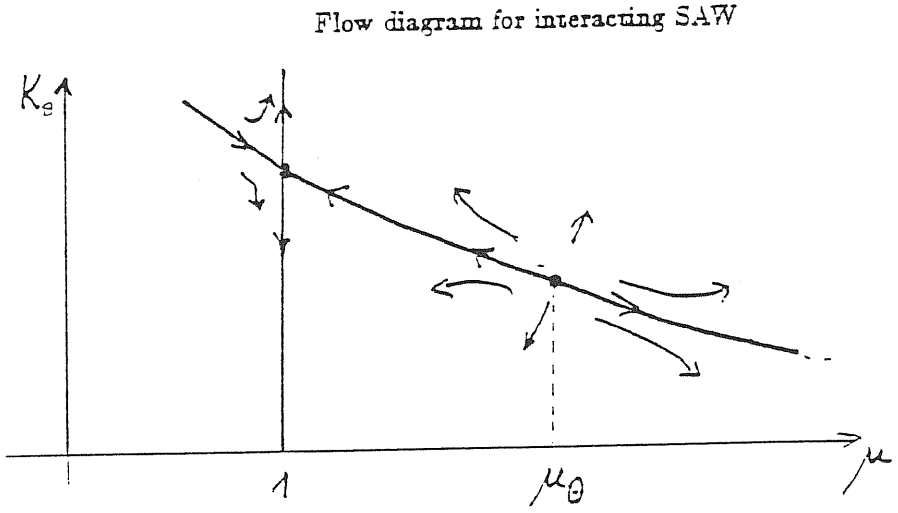

fig 15

which shows three fixed points: The first for $\mu = 1$ corresponds to $T \longrightarrow \infty$, that is to non-interacting SAWs. The second for $\mu = \mu_0$ corresponds to $T = T_\Theta$, the Flory

temperature, with a size exponent $\nu_\Theta \cong 0.57$. The third fixed point is at $\mu = \infty$, and corresponds to a collapsed chain.

Another real space renormalisation approach to the Θ-point problem in dimension $d = 2$ was proposed by Jug [7], which has the advantage of being simple enough for extension to three dimensions, and also to inhomogeneous environment and polymer composition. This model and an extended version which includes surface interactions are presented in the next section.

3.1 Self-Avoiding – Self-Attracting Model for the Θ–Point.

I will present here the model introduced by Jug[7] for the Θ-point problem, with some small and globally irrelevant numerical modifications due to the fact that a computer program has been used to generate and classify cell configurations, allowing for a complete account of all the random-walk configurations required.

To start with, we introduce a two dimensional triangular lattice and we define bare and renormalised cells with rescaling factor $b = 2$:

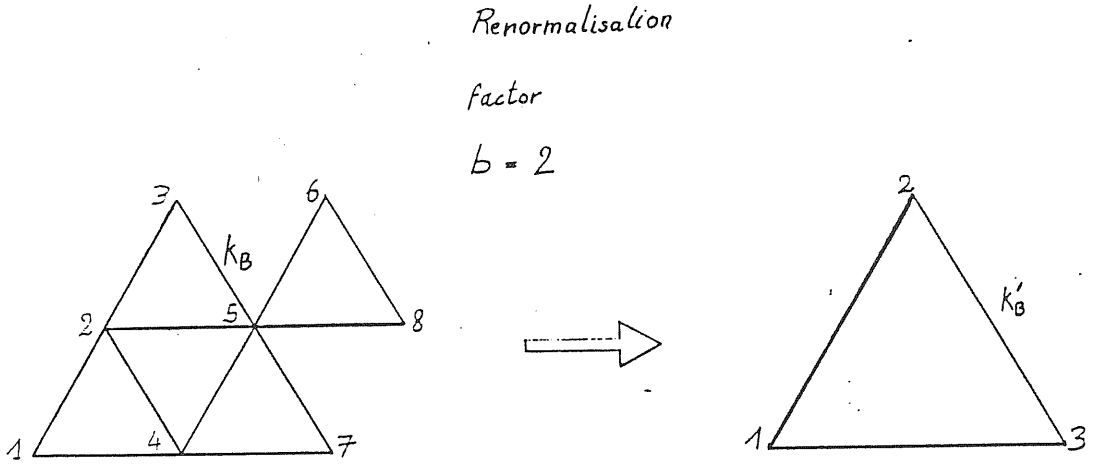

(a) Bare cell (b) Renormalised cell

fig.16

A polymer configuration will be represented by a walk on the lattice cell and characterized by a fugacity k_B for each step on the bare cell, whilst a step on the renormalised cell will be attributed a fugacity k'_B .

We then need to make a distinction between polymer chains at $T > T_\Theta$ and at $T < T_\Theta$. Thus a swollen polymer chain will be represented by SAW configurations and a collapsed chain by configurations with at least one two-body contact.

In order to avoid unphysical densities the three-body contacts, which are possible in a triangular lattice, must be excluded. From the mean field approach presented in section 1.3 we actually know that the Flory excluded volume parameter v determines the two-body interactions (see eq.(12)). When we have $v > 0$ these interactions are repulsive and we have a swollen chain, whereas for $v < 0$ they are attractive. In such a case the chain is in a collapsed state and only higher order repulsive interactions avoid unphysical densities.

So the condition of excluding configurations with three-body contacts is a practical way of taking into account the three-body repulsive interactions.

Extending the scheme presented in section 2.2, we evaluate the partition functions for the two types of walks :

$$Z^B_{SAW}(k_B) = \sum_{n_B} C_{SAW}(n_B) \cdot k_B^{n_B} \tag{54}$$

$$Z^B_{G}(k_B) = \sum_{n_B} C_{G}(n_B) \cdot k_B^{n_B} \tag{55}$$

The index B, stands for *bulk*.

The coefficients $C_{SAW}(n_B)$ and $C_G(n_B)$ are the numbers of SAW and Globule configurations, respectively, made up of n_B steps.

However, in order to minimize the error introduced by the finite-size of the lattice cell approximation, we apply a number of (arbitrary) rules of more or less intuitive origin.

Thus, with the scope of obtaining a sufficiently complete connectivity between the walks in the neighboring cells of an infinite lattice, we consider only the configurations that span our bare cell. The spanning configurations are those which, on figure 16a, start at site 1 and contain sites 3 and/or 6 .

In a similar way, we construct the partition functions for the renormalised cell considering configurations, in figure 16b, that start at site 1 and contain site 2 .

The renormalisation transformations in the one dimensional parameter space are, for SAWs and globules respectively,

$$Z^B_{SAW}(k_B) = Z'^B_{SAW}(k'_B) \tag{56}$$

$$Z^B_G(k_B) = Z'^B_G(k'_B) \tag{57}$$

which leads to

SAW :	$k_B^{*SAW} \cong 0.316$	$\nu_B^{SAW} \cong 0.782$
Globule :	$k_B^{*G} \cong 0.494$	$\nu_B^{G} \cong 0.529$

Considering the very small (2 x 2) cells used, we can say that the results are quite encouraging since we expect $\nu_B^{SAW} \cong 3/4$ and $\nu_B^G = 1/2$ (compact two dimensional structure).

In order to describe the coil-globule transition, it is necessary to introduce a new parameter f, which represents the probability that one of the possible sites in the cell is the host of a two body contact. We can then set up a new bulk partition function, which is consistent with the previous two, in the sense that for $f = 0$ and $f = 1$ we find again the SAW and globular limit cases.

However, we must first perform the following decomposition of the globule partition function:

$$Z^B_G(k_B) = \sum_{m=1}^{4} Z^B_{G_m}(k_B) \tag{58}$$

with

$$Z_{G_m} = \sum_{n_B} C_{G_m}(k_B) \cdot k_B^{n_B} \tag{59}$$

where $C_{G_m}(k_B)$ denotes the number of n_B-step configurations, with m two-body contacts. In the small cell we have considered, m cannot be greater than four. On figure 16 the sites liable to host a monomer-monomer contact are sites one, two, four, and five.

The Θ-point partition function will be the weighted sum of SAW and globule partition functions:

$$Z_{\Theta}^{B}(k_B, f) = (1-f)^4 \cdot Z_{SAW}^{B}(k_B) + \sum_{m=1}^{4} f^m \cdot Z_{G_m}^{B}(k_B) \tag{60}$$

$(1-f)^4$ is the probability of no contact, and thus is a weight for the configurations in Z_{SAW}^{B} . f^m is the probability of m self- contacts and is therefore used to weight the configurations in $Z_{G_m}^{B}$.

In the renormalised cell, the maximum number of contacts is just one (the origin). Then, denoting the contact probability by f' we have:

$$Z_{\Theta}^{'B}(k'_B, f') = (1-f') \cdot Z_{SAW}^{'B}(k_B) + f' \cdot Z_{G}^{'B} \tag{61}$$

Again imposing the conservation of the cell partition functions under renormalisation

$$Z_{\Theta}^{'B}(k'_B, f') = Z_{\Theta}^{B}(k_B, f) \tag{62}$$

we obtain implicitly a recursion relation:

$$k'_B = k'_B(k_B, f) \tag{63}$$

In order to determine a fixed point (k_B^*, f^*) we need a second one:

$$f' = f'(k_B, f) \tag{64}$$

But $f' = N/D$, where N is the number of bare cell configurations, that can give rise to a renormalised configuration with a two-body contact. D is the total number of all configurations. Naturally, each configuration in N and D must be weighted by a fugacity as well as by a probability factor. We then write:

$$f' = \frac{\sum_{m=1}^{4} f^m \cdot (1-f)^{4-m} \cdot Z_{Gm}^B}{(1-f)^4 \cdot Z_{SAW}^B + \sum_{m=1}^{4} f^m \cdot (1-f)^{4-m} \cdot Z_{Gm}^B} \tag{65}$$

The weighting probability factor has been chosen in such a way that f' is a normalised probability. We can actually check that for $f = 0$ we have $f' = 0$, and for $f = 1$ we have $f' = 1$.

Introducing $f = f' = 1$ and $f = f' = 0$ in the equation (65), it is easy to see that we obtain the recursion relation for the globule and for the SAW case, respectively.

From equations (62) and (65), it is possible, using Newton's method, to find the fixed point.

The eigenvalues λ_B and λ_f of the jacobian matrix of the renormalisation transformation, evaluated at the fixed point (k_B^*, f^*) , are related to the critical exponents ν_B, ν_f through:

$$\nu_i^{\Theta} = \frac{\ln b}{\ln \lambda_i} , \qquad i = B, f$$

ν_B^{Θ} governs the asymptotic behaviour of the characteristic size near the Θ-point. A slightly more detailed description of this procedure will be given in the next section, where we will tackle the problem of the coil globule transition near a wall. Here, we just note that we obtain $\nu_B^{\Theta} \cong 0.513$.

3.2 Extension of the model to include Wall Interactions.

In 1983, Kremer [8] introduced the first real-space renormalisation group approach to the adsorption of a simple self-avoiding chain in dimensions $d = 2$ and $d = 3$. He used a square lattice and a cell-to-cell renormalisation very similar to the one proposed by de Queiroz and Chaves [19] and briefly described in section 2.2. The fundamental difference is that one side of the cell was considered to represent a surface, and therefore each step on this "surface" was attributed a different fugacity k_S, giving rise to a two-parameters renormalisation transformation defined by:

$$Z^{S}_{SAW}(k_B, k_S) = Z'^{S}_{SAW}(k'_B, k'_S) \tag{66a}$$

$$Z^{B}_{SAW}(k_B) = Z'^{B}_{SAW}(k'_B) \tag{66b}$$

The equation (66a) concerns cells near the surface, whereas the equation (66b) is the well known bulk renormalisation condition.

Kremer found

$$\nu_B^{SAW} \cong 0.73$$
$$\nu_S^{SAW} \cong 1.36$$

where ν_S^{SAW} is related to the characteristic length perpendicular to the surface by

$$\langle R^2 \rangle_{\perp}^{1/2} \sim \mid T - T_a \mid^{-\nu_S}$$

with T_a the adsorption desorption temperature as explained in section 1.4.

The model described in section 3.1, can also be modified by introducing a surface.The bare and renormalised cells are as in figure 17:

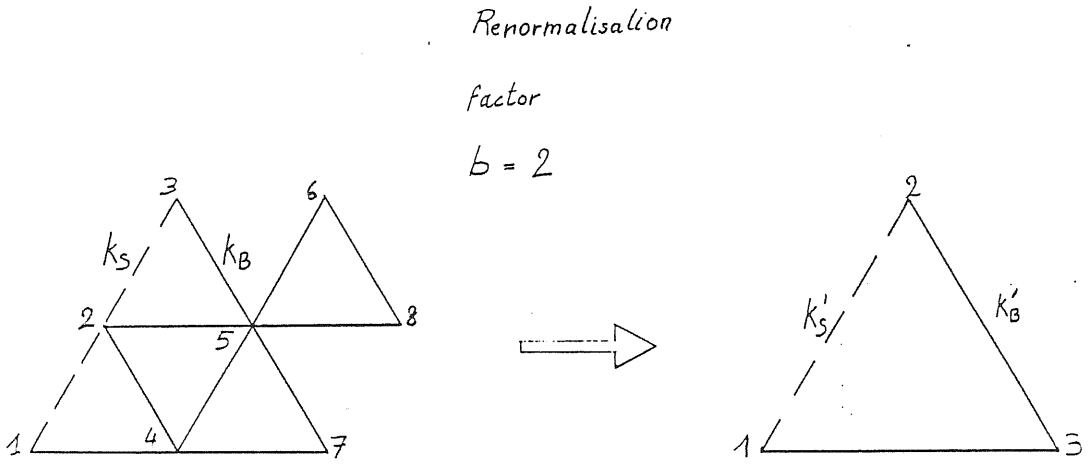

(a) Bare cell (b) Renormalised cell

fig.17

with a fugacity k_B for steps in the bulk, and k_S for steps on the surface.

We then proceed exactly in the same way as in section 3.1, but we must introduce another fairly arbitrary rule, in order to control the adsorption rate of the chain. We then decide that an adsorbed chain will be renormalised into another adsorbed chain, only if at least a finite fraction $1/x$ of its length belongs to the surface.

The choice of x is arbitrary, even if there is obviously a value x_{max} such that, for every $x \geq x_{max}$ the surface partition function will contain all the configurations which have at least one step on the surface.

For instance, let us consider the self-avoiding configurations on the bare cell (fig.17a): The longer SAW that we can draw has 6 steps. Only one of them is on the surface. Denoting by n_B the number of steps in the bulk, and by n_S those on the surface, we have $n_B + n_S = 6$, and $n_S = 1$. The adsorbed fraction is:

$$\frac{n_S}{n_B + n_S} = \frac{1}{x} \tag{67}$$

with $1/x = 1/6$

Because the configuration we are talking about is the less adsorbed SAW we can construct, we see that for each choice $x \geq 6 = x_{max}$, all the other walks satisfy our rule, which can now be stated:

$$\frac{n_S}{n_B + n_S} \geq \frac{1}{x} \tag{68}$$

Summarizing, we will say that the greater x we choose the more weakly adsorbed configurations will be allowed to contribute to the partition function. The result will be a statistically less adsorbed chain.

It must also be noticed that on the cell, Globular walks can be longer than SAW. Therefore we will have:

$$x_{max}(\text{Globule}) \; > \; x_{max}(\text{Self} - \text{Avoiding}) \tag{69}$$

In choosing x, we must be consistent by taking $x \leq x_{max}(SAW)$, in order to have identical "adsorption properties" of the surface in globular and SAW phases.

Combining the models of Jug and Kremer, it is straightforward to write the following renormalisation recursion relations:

$$Z_{\Theta}^{'S_{1/x}}(k'_B, k'_S, f') = Z_{\Theta}^{S_{1/x}}(k_B, k_S, f) \tag{70a}$$

$$Z_{\Theta}^{'B}(k'_B, f') = Z_{\Theta}^{B}(k_B, f) \tag{70b}$$

$$f' = \frac{\sum_{m=1}^{4} f^m \cdot (1-f)^{4-m} \cdot Z_{Gm}^{S_{1/xmax}}}{(1-f)^4 \cdot Z_{SAW}^{S_{1/xmax}} + \sum_{m=1}^{4} f^m \cdot (1-f)^{4-m} \cdot Z_{Gm}^{S_{1/xmax}}} \tag{70c}$$

with:

$$Z_{\Theta}^{S_{1/x}}(k_B, k_S, f) = (1-f)^4 \cdot Z_{SAW}^{S_{1/x}} + \sum_{m=1}^{4} f^m \cdot Z_{Gm}^{S_{1/x}} \tag{71a}$$

$$Z_{\Theta}^{'S_{1/x}}(k'_B, k'_S, f') = (1-f') \cdot Z_{SAW}^{'S_{1/x}} + f' \cdot Z_{G}^{'S_{1/x}} \tag{71b}$$

$$Z_{\Theta}^{B}(k_B, f) = (1-f)^4 \cdot Z_{SAW}^{B} + \sum_{m=1}^{4} f^m \cdot Z_{Gm}^{B} \tag{71c}$$

$$Z_{\Theta}^{'B}(k'_B, f') = (1-f') \cdot Z_{SAW}^{'B} + f' \cdot Z_{G}^{'B} \tag{71d}$$

and

$$Z_{SAW}^{S_{1/x}}(k_B, k_S) = \sum_{n_B, n_S} C_{SAW}^{2\times 2}(n_B, n_S, x) \cdot k_B^{n_B} \cdot k_S^{n_S} \tag{72a}$$

$$Z_{G_m}^{S_{1/x}}(k_B, k_S) = \sum_{n_B, n_S} C_{G_m}^{2\times 2}(n_B, n_S, x) \cdot k_B^{n_B} \cdot k_S^{n_S} \tag{72b}$$

$$Z_{SAW}^{'S_{1/x}}(k'_B, k'_S,) = \sum_{n_B, n_S} C_{SAW}^{1\times 1}(n_B, n_S, x) \cdot k_B^{'n_B} \cdot k_S^{'n_S} \tag{72c}$$

$$Z_{G_m}^{'S_{1/x}}(k'_B, k'_S) = \sum_{n_B, n_S} C_{G_m}^{1\times 1}(n_B, n_S, x) \cdot k_B^{'n_B} \cdot k_S^{'n_S} \tag{72d}$$

$$Z_{SAW}^{B}(k_B) = \sum_{n_B} C_{SAW}^{2\times 2}(n_B) \cdot k_B^{n_B} \tag{72e}$$

$$Z_{G_m}^{B}(k_B) = \sum_{n_B} C_{G_m}^{2\times 2}(n_B) \cdot k_B^{n_B} \tag{72f}$$

$$Z'^{B}_{SAW}(k'_B) = \sum_{n_B} C^{1\times 1}_{SAW}(n_B) \cdot k'^{n_B}_B \tag{72g}$$

$$Z'^{B}_{G_m}(k'_B) = \sum_{n_B} C^{1\times 1}_{G_m}(n_B) \cdot k'^{n_B}_B \tag{72h}$$

Since a SAW is equivalent to a zero contact "globule" walk, we have:

$$C_{SAW} = C_{G0}, \qquad (m = 0) \tag{73}$$

So $C^{a\times b}_{G_m}(n_B, n_S, x)$ is the number of walk-configurations on a $(a \times b)$ surface-cell with n_B steps in the bulk, n_S steps on the surface, with m two-body (monomer-monomer) contacts, and an adsorbed fraction $n_S/(n_B + n_S)$ greater than $1/x$.

Similarly $C^{a\times b}_{G_m}(n_B)$ is the number of configurations in a bulk cell with n_B steps and m two-body contacts.

We then realize that the first step in the determination of the critical exponents and phase diagram is to calculate the coefficients $C^{a\times b}_{G_m}(n_B, n_S, x)$ and $C^{a\times b}_{G_m}(n_B)$. This has been performed with the help of a computer program described in appendix [7.1].

Next, we need to find a fixed point $\vec{\mu}^* = (k^*_B, k^*_S, f^*)$ for the 3-dimensional parameter space transformation, defined by the equations (70a), (70b), and (70c).

In order to simplify the notations a little, we rewrite these three equations:

$$F_l(\vec{\mu}') = F_r(\vec{\mu}) \tag{74a}$$

$$G_l(\vec{\mu}') = G_r(\vec{\mu}) \tag{74b}$$

$$H_l(\vec{\mu}') = H_r(\vec{\mu}) \tag{74c}$$

and we define:

$$F(\vec{\mu}^*) = F_l(\vec{\mu}^*) - F_r(\vec{\mu}^*) = 0 \tag{75a}$$

$$G(\vec{\mu}^*) = G_l(\vec{\mu}^*) - G_r(\vec{\mu}^*) = 0 \tag{75b}$$

$$H(\vec{\mu}^*) = H_l(\vec{\mu}^*) - H_r(\vec{\mu}^*) = 0 \tag{75c}$$

where $\vec{\mu} = \vec{\mu}' = \vec{\mu}^*$.

To find the fixed points, we use Newton's method which consists in generating a series $\vec{\mu}_i = (k_B^i, k_S^i, f^i)$ of converging approximations, starting from an initial guess $\vec{\mu}^0 = (k_B^0, k_S^0, f^0)$.

First of all we approximate the equations (75a), (75b), and (75c) by a linear development in (k_B^0, k_S^0, f^0) :

$$F(\vec{\mu}^0) \cong \vec{\nabla}\ F(\vec{\mu}^0) \cdot \delta\vec{\mu} = 0 \tag{76a}$$

$$G(\vec{\mu}^0) \cong \vec{\nabla}\ G(\vec{\mu}^0) \cdot \delta\vec{\mu} = 0 \tag{76b}$$

$$H(\vec{\mu}^0) \cong \vec{\nabla}\ H(\vec{\mu}^0) \cdot \delta\vec{\mu} = 0 \tag{76c}$$

with $\delta\vec{\mu} = (k_B^1 - k_B^0, k_S^1 - k_S^0, f^1 - f^0)$.

The three equations above are nothing but a linear system, that can be solved for $\vec{\mu}^1 = (k_B^1, k_S^1, f^1)$. Considering $\vec{\mu}^1$ as the new guess, we repeat the procedure until $| \vec{\mu}^{i+1} - \vec{\mu}^i | < \varepsilon$, ε being the precision required.

At this point, if it were possible to put the equations (74a), (74b), and (74c) in the form:

$$k'_B = k'_B(k_B, k_S, f) \tag{77a}$$

$$k'_S = k'_S(k_B, k_S, f) \tag{77b}$$

$$f' = f'(k_B, k_S, f) \tag{77c}$$

the jacobian matrix:

$$\left.\frac{\partial \vec{\mu}'}{\partial \vec{\mu}}\right|_{\vec{\mu}^*} = \left.\frac{\partial(k'_B, k'_S, f')}{\partial(k_B, k_S, f)}\right|_{\vec{\mu}^*} \tag{78}$$

would be easily calculated and diagonalised.

Unfortunately, this is not possible, and in order to find the jacobian matrix elements, we must return to the equations (74a), (74b), (74c), and derive each one with respect to k_B, k_S, and f. We then obtain a system of nine equations, that we formally write:

$$\frac{\partial F_l}{\partial \vec{\mu}'} \cdot \left.\frac{\partial \vec{\mu}'}{\partial \vec{\mu}}\right|_{\vec{\mu}^*} = \left.\frac{\partial F_r}{\partial \vec{\mu}}\right|_{\vec{\mu}^*} \tag{79a}$$

$$\frac{\partial G_l}{\partial \vec{\mu}'} \cdot \left.\frac{\partial \vec{\mu}'}{\partial \vec{\mu}}\right|_{\vec{\mu}^*} = \left.\frac{\partial G_r}{\partial \vec{\mu}}\right|_{\vec{\mu}^*} \tag{79b}$$

$$\frac{\partial H_l}{\partial \vec{\mu}'} \cdot \left.\frac{\partial \vec{\mu}'}{\partial \vec{\mu}}\right|_{\vec{\mu}^*} = \left.\frac{\partial H_r}{\partial \vec{\mu}}\right|_{\vec{\mu}^*} \tag{79c}$$

Solving for the nine unknowns $\left.\frac{\partial \vec{\mu}'}{\partial \vec{\mu}}\right|_{\vec{\mu}^*}$, we obtain the jacobian matrix and, diagonalising it, we calculate the eigenvalues λ_B, λ_S, and λ_f, and then the critical exponents near the fixed point $\vec{\mu}^*$.

Needless to say, such renormalisation procedure has several fixed points. As we are going to see in the next section, some of them are unphysical or of little interest, others are representative of a particular physical situation.

4.1 Fixed Points and their Interpretation.

As explained in the previous chapter, our model can describe the adsorption of polymer chains in their three distinct possible phases: SAW, Globule, and Θ-point. For each phase there is an adsorption-desorption fixed point, with $f = 0$, $f = 1$, and $f = f^*$ respectively.

Furthermore, it is very easy to eliminate the surface, using for the coefficients $C_{G_m}(n_B)$ in equation (59) the following relation:

$$C_{G_m}^{a\times b}(n_B) = \sum_{\substack{n=1 \\ n=n_B+n_S}}^{\infty} C_{G_m}^{a\times b}(n_B, n_S, x=\infty) \tag{80}$$

We then obtain the model of Jug presented in section 3.1 for the bulk situation.

The results obtained in section 3.1 by means of the exact numerical enumerations are herewith summarized :

Characteristics of a chain far from surface (bulk):

Self-Avoiding phase or swollen chain:

`Fixed point:`	$k_B^{*SAW} \cong 0.316$	$f^{*SAW} = 0.000$
`Critical exponent:`	$\nu_B^{SAW} \cong 0.782$	

Globule phase or collapsed chain:

`Fixed point:`	$k_B^{*G} \cong 0.494$	$f^{*G} = 1.000$
`Critical exponent:`	$\nu_B^{G} \cong 0.529$	

Θ-point phase or chain at the Flory compensation temperature:

Fixed point:	$k_B^{*\Theta} \cong 0.520$	$f^{*\Theta} = 0.812$
Critical exponents:	$\nu_B^{\Theta} \cong 0.513$	$\nu_f^{\Theta} \cong 1.322$

Characteristics of a chain near a surface:

Self-Avoiding phase or swollen chain:

Fixed point:	$k_B^{*SAW} \cong 0.316$	$k_S^{*SAW} \cong 0.377$	$f^{*SAW} = 0.000$
Critical exponents:	$\nu_B^{SAW} \cong 0.782$	$\nu_S^{SAW} \cong 1.636$	

Globule phase or collapsed chain:

Fixed point:	$k_B^{*G} \cong 0.494$	$k_S^{*G} \cong 0.638$	$f^{*G} = 1.000$
Critical exponents:	$\nu_B^{G} \cong 0.529$	$\nu_S^{G} \cong 1.39$	

Θ-point phase or chain at the Flory compensation temperature:

Fixed point:	$k_B^{*\Theta} \cong 0.528$	$k_S^{\Theta} \cong 0680$	$f^{*\Theta} = 0.759$
Critical exponents:	$\nu_B^{\Theta} \cong 0.513$	$\nu_S^{\Theta} \cong 1.610$	

Comments:

a) First of all we consider chains in the bulk, and we compare the values of critical exponents in the original work [7] with those presented above.

We have $\nu_B^{SAW} \cong 0.782$, instead of 0.787 . The new value is closer to the expected value 0.75 .

Surprisingly, the situation is less satisfactory for the Globule exponent, since we have $\nu_B^{G} \cong 0.529$ against 0.508 and we know that the expected value should be $1/2$.

For the Θ-point, the value $\nu_B^{\Theta} \cong 0.513$, instead of 0.494 seems to be in a slightly better agreement with some previous estimates quoted by Jug [7].

I conclude that the new set of configurations used in this work does not modify the situation significantly, and that the advantages (simplicity and correct overall predictions) and the disadvantages (not very precise numerical values) are confirmed.

b) We now look at the results for chains near a surface, and we must first specify that the results given above correspond to chains with a minimum adsorbed fraction $1/x = 1/6$.

The reason for this choice, as explained in section 3.2, lies in the necessity of being consistent and to have identical "adsorption properties" in globular and SAW phases. We notice since now that, due to the smallness of the cells considered, we cannot impose the same "adsorption" in bare and renormalised cells. This is certainly an important source of error.

SAW phases. Let us now consider the SAW phase. In the literature one often defines the so-called cross-over exponent $\varphi = \frac{\nu_B}{\nu_S}$ which is related to the asymptotic fraction N_S/N of monomers at the surface. In particular at $T = T_a$, we have [9]:

$$\frac{N_S}{N} \propto N^{\varphi - 1} , \qquad N \longrightarrow \infty \tag{81}$$

From our values of ν_S^{SAW} and ν_B^{SAW} , it turns out that $\varphi^{SAW} \cong 0.478$. This value is quite encouraging since, following a recent (1989) work of Burkhardt, Eisenriegler, and Guim [20], the presumed exact value is $\varphi = 1/2$.

Incidentally, we note that the exactly calculated value of φ for ideal chain is also $\varphi = 1/2$ [9]. This fact seems to give rise to some controversial interpretations. The simples hypothesis is that the surface attraction exactly compensates the monomer-monomer repulsive interactions.

Globular phase. From a recent work (unpublished) by Bouchaud and Vannimenus[10], the value $1/2$ seems to be an upper bound for φ which should be reached by globule chains.

From our values of ν_B^G and ν_S^G , we obtain $\varphi \cong 0.38$ which is much less satisfactory than for the SAW phase! Nevertheless the values of ν_B^G and ν_S^G are not far from their expected values $1/2$, and $3/2$ respectively.

Θ-point. About the Θ-point presented above, we can say our work presents the first evidence of the existence, with a real space calculation, of a multicritical point, where a bulk collapse transition and a surface adsorption transition coexist.

In the above quoted work, J. Vannimenus, and E. Bouchaud have found such a multicritical point but on a deterministic fractal space in which the renormalisation recursion can be constructed exactly.

c) We now compare bulk and surface results.

The first aspect that we note is that the presence of a surface does not modify the values of ν_B^{SAW} , ν_B^G , and ν_B^Θ . This exponents can be related to the dimensions of the chain in the direction parallel to the surface.

The second, and certainly most important remark that we can do, concerns the values of $f^{*\Theta}_{\text{surface}}$, and $f^{*\Theta}_{\text{bulk}}$. We find :

$$f^{*\Theta}_{\text{surface}} \; < \; f^{*\Theta}_{\text{bulk}} \tag{82}$$

The variable f being the probability of a monomer-monomer contact on a lattice site, it is likely that it will depend on temperature, for example through:

$$f \approx 1 - \mathrm{e}^{E/kT} \tag{83}$$

where $E < 0$ is the relative attraction energy between two monomers.

This dependence assures that for $T \longrightarrow \infty$, we have $f \longrightarrow 0$, and for $T \longrightarrow 0$, we have $f \longrightarrow 1$, as it is shown in figure 18:

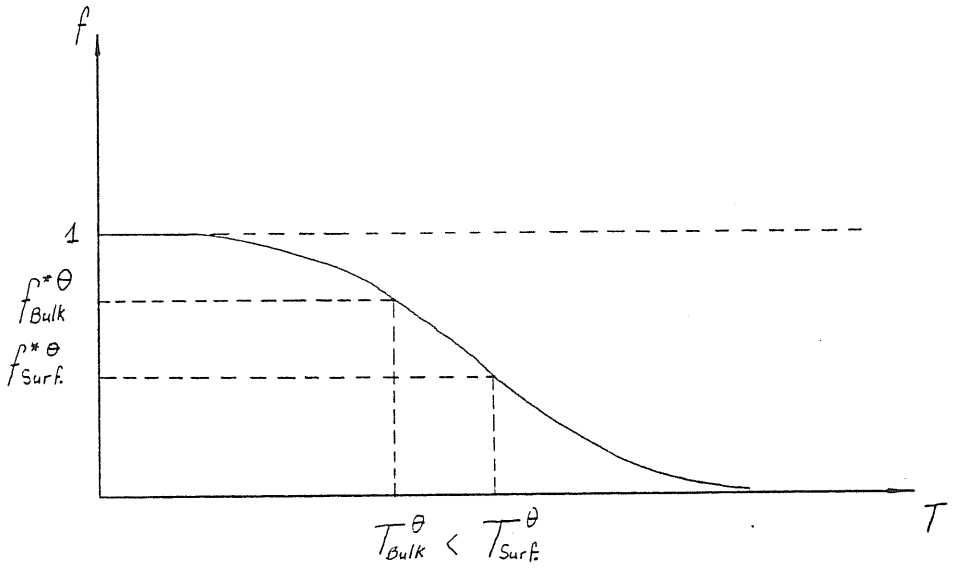

fig.18

Therefore,*the presence of a surface increases the coil-globule transition temperature* Θ*!* This highly non-trivial result should be of some biological relevance. For instance, at physiological temperatures, a biopolymer could be in a coil state when in the cytoplasma, and in a collapsed functional state when adsorbed on the cell membrane. There are certainly many situations in which we can imagine that such a mechanism holds, since the monomer-monomer contact probability can be modified not only by a temperature variation, but also by any other factor that changes the monomer-solvent, or the monomer-monomer interactions.

The coupling should certainly also function in the opposite way. This mean that instead of a coil to globule transition induced by adsorption, we should also observe desorption induced by a globule to coil transition, or adsorption induced by a coil to globule transition. This last mechanism could concern proteins with one part embedded in the membrane, and another which moves freely in the vicinity of the

membrane. If now a change in the environmental conditions produces a collapse of the free tail, the above coupling could induce an adsorption transition.

The important feature is that, according to our model, the very short-range attractive forces between the surface and the "protein" (a monomer is adsorbed only if it lies on the surface) can induce, through cooperative processes, such an important change in the "protein" conformation as a coil-globule transition.

4.2 Phase diagram

If we consider the one dimensional parameter space renormalisation briefly described in section 2.2, we can see that there are three fixed points for $k_B = 0$, $k_B = 1$, and $k_B = k_B^*$. The physical interpretation of these fixed points is useful for the understanding of the phase diagrams presented in figure 19. The recursion relation corresponding to figure 13 faithfully rescales an empty lattice $(k_B = 0)$ into another empty lattice $(k'_B = 0)$. Furthermore, for every $k_B < k_B^*$, we have $k'_B < k_B$. Thus, after an infinite number of renormalisations, we reach the limit $k_B = 0$.

This means that for $k_B < k_B^*$, the SAWs are finite in length, and they shrink upon each renormalisation.

For $k_B > k_B^*$, we have $k'_B > k_B$, and we reach, after an infinite number of renormalisations, the fixed point $k_B = 1$, which means that every site of the lattice is visited and the SAW densely packs the lattice.

We will say that $k_B = 1$ and $k_B = 0$ are trivial fixed points in the sense that they correspond to evident self-similar situations, i.e. empty lattice and full lattice, whereas $k_B = k_B^*$ corresponds to an intermediate non-trivial self-similar situation, that can be associated with infinite SAWs.

Thus, as shown in sections 2.1 and 2.2, the study of the properties of the renormalisation function near the fixed point, gives us information about the geometrical properties of very long SAW chains.

We now return to our three parameter real space renormalisation. In section 4.1, we have given the coordinates of the three non-trivial fixed points which should be located in a cubic renormalisation flow diagram, or phase diagram. Just to give an idea of this renormalisation flow, I choose to present in figure 19 the three plane sections (k_B = constant) that contain the three non-trivial fixed points presented in section 4.1.

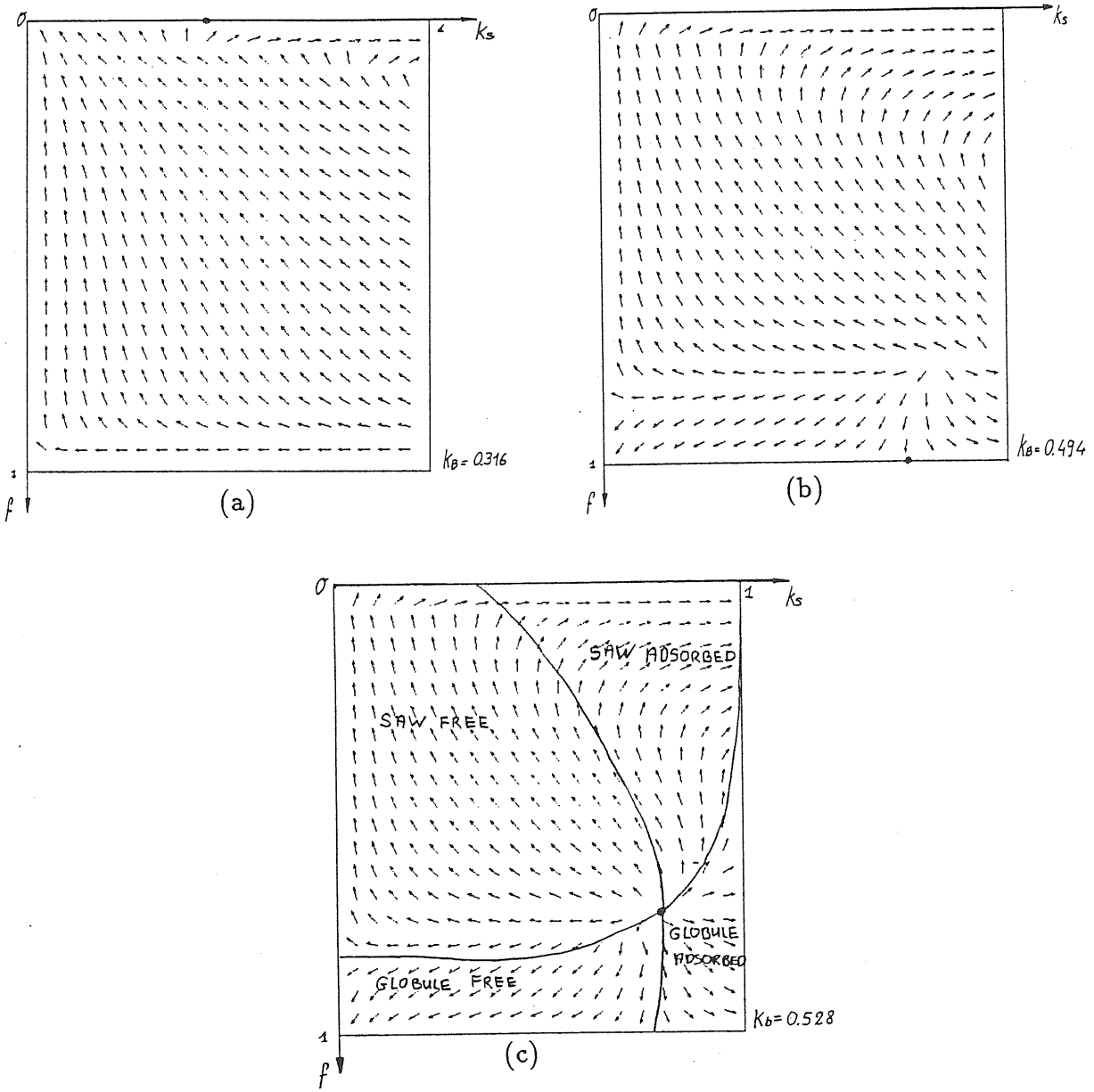

fig.19

On the figure 19(a), we can see, for $f = 0$ and $k_B \cong 0.316$, the adsorption-desorption

fixed point at $k_S = 0$. We note that there is no fixed point for $k_S = 1$.

So self-similarity occurs when there is no adsorption, and in a less trivial case, in which, infinite, slightly adsorbed chains make loops of any size, like in figure 20.

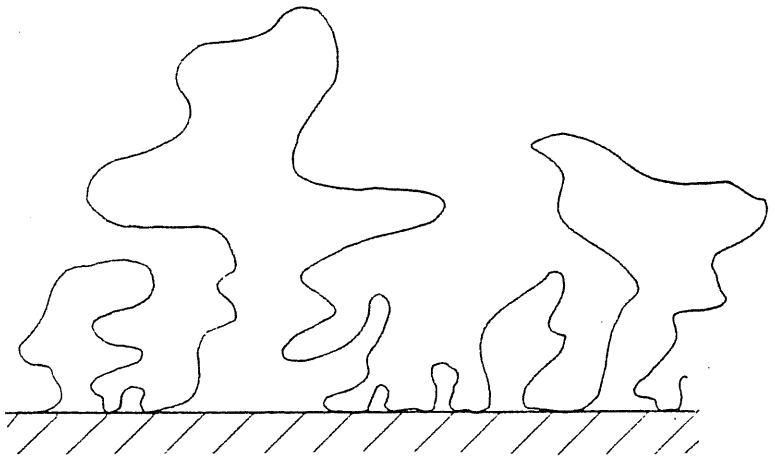

fig.20

This situation is associated with adsorption-desorption transition. When the chain is adsorbed, there is no more self-similarity, because the adsorbed layer has a finite size.

In figure 19(b), the situation is very similar: Now, $k_B \cong 0.494$ and we have again two fixed points but for $f = 1$, which correspond to two situations in which the self-similarity occurs. Again, we have a trivial one (free surface), and a less trivial which corresponds to the globule adsorption transition.

In figure 19(c), we have the most interesting situation for $k_B \cong 0.528$, where we can see the multicritical point, which corresponds to an adsorption-desorption transition of a Θ-chain. I have drawn on the same plane the fixed point which corresponds to a free surface for Θ-chains, but in reality, this fixed point occurs for a slightly lower value of k_B, more precisely for $k_B \cong 0.512$.

This is in contrast with the SAW and globule cases for which the trivial fixed points occur for the same value of k_B, than the adsorption-desorption point. This fact can be interpreted like another manifestation of the coupling between the two different transitions. On figure 19(c), I have also tried to draw the critical lines, which separate the different phases.

This separation looks a little arbitrary but can be better understood from the figure

21, in which I draw all the fixed points I could find, and the two crossed critical lines which separate the four phases: free SAW, free Globule, adsorbed SAW, and adsorbed Globule.

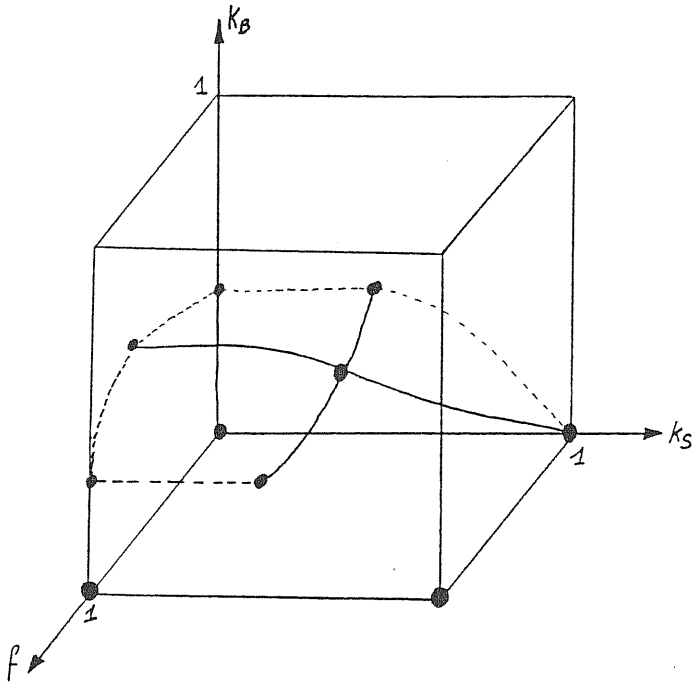

fig.21

The lines on figure 19(c) are the "projections" of the two critical lines of figure 21 on the plane $k_B \cong 0.528$.

In order to obtain much more accurate exponents and confirmation of the shift in $f^{*\Theta}$, it is necessary to consider bigger cells. To do this I developed a computer program, which is presented in appendix (7.1). Unfortunately, the generation of globular configurations is still not in full order and I must forego the presentation of the results for globular and Θ-point phases. This is unfortunate, as the results for SAW phases are really remarkable. We have performed two renormalisations. The first one is from a 3×3 towards a 1×1 cell whereas the second is from a 3×3 towards a 2×2, as seen in figure 22.

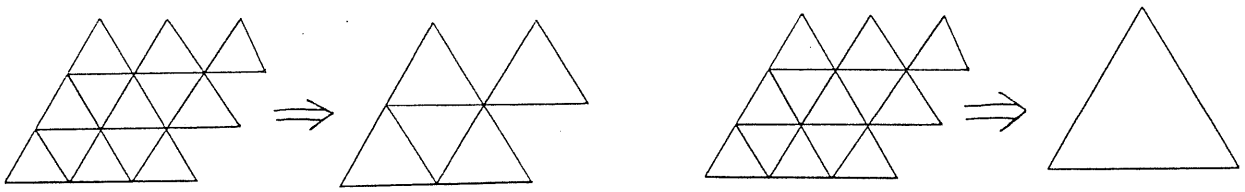

fig.22

The details of SAW configurations are given in appendix (7.3).

The fixed point, and the relative critical exponents are as follows:

$3 \times 3 \longrightarrow 1 \times 1$ *cell renormalisation:*

`Fixed point:`	$k_B^{*SAW} \cong 0.298$	$k_S^{*SAW} \cong 0.413$	$f^{*SAW} = 0.000$
`Critical exponents:`	$\nu_B^{SAW} \cong 0.772$	$\nu_S^{SAW} \cong 1.548$	

$3 \times 3 \longrightarrow 2 \times 2$ *cell renormalisation:*

`Fixed point:`	$k_B^{*SAW} \cong 0.284$	$k_S^{*SAW} \cong 0.453$	$f^{*SAW} = 0.000$
`Critical exponents:`	$\nu_B^{SAW} \cong 0.756$	$\nu_S^{SAW} \cong 1.491$	

The most surprising result is the excellent accuracy obtained with larger but still small cells. Particularly for the $3 \times 3 \longrightarrow 2 \times 2$ renormalisation we are very near the expected values $\nu_B^{SAW} \cong 0.750$ and $\nu_S^{SAW} \cong 1.500$. The situation is consequently very satisfactory also for the cross-over exponent $\varphi = \nu_S/\nu_B \cong 0.508$.

I believe these are the best results obtained till now for the adsorption-desorption transition of coil chains. One reason for such an improvement in accuracy for critical exponents values is certainly the possibility with a $3 \times 3 \longrightarrow 2 \times 2$ renormalisation procedure, to impose the same adsorption properties in bare and renormalised cells. To do this, we must choose $\frac{1}{x} = \frac{1}{6}$ for the minimum fraction adsorbed.

6. CONCLUSION AND OUTLOOK

In this work, I have presented a novel real space renormalisation scheme for surface adsorption-desorption transition of polymer chains in their three possible phases: coil, globule, and Θ-point. The main result is the discovery of the existence of a multicritical point, in which the adsorption-desorption transition coexists with a coil-globule transition. Comparing the fixed point related to the coil-globule transition in both surface and bulk cases, I conclude that a coupling must occur between adsorption-desorption and coil-globule transitions.

I also have tried to briefly point out the great importance that such a coupling may have for understanding a large class of biological phenomena involving proteins and membranes. For coil or SAW phases, one could improve the accuracy of the critical exponent numerical values by using a slightly larger renormalisation cell. The results are rather spectacular since we are very close to the expected values $\nu_B^{SAW} = 3/4$, and $\nu_S^{SAW} = 3/2$, and it is likely that the present results are the best currently available.

In chapter 1 and 2, I have tried to justify the construction of this model, and to present all the necessary background for understanding it.

Once again, one should stress that what has been presented here is only a very crude model for proteins, especially because the distribution of hydrophilic and hydrophobic residues along the chain has not been taken into account.

The next step towards a more realistic protein model will be precisely the introduction of such a distribution. It will certainly be very interesting to try to introduce a cell membrane, which may be modelled by attributing a different two-body contact probability for each of the two regions of (lattice) space defined by the fluid interface.

But first of all, it is necessary to obtain correct globular configurations by a suitable modification of the enumerating computer program presented in appendix (7.1).

It should be stressed at the end of this work that although the model and analysis has been carried out for a two-dimensional protein folding model, so that the adsorption is at a line, the extension to the realistic three dimensional model where the adsorption is at a

surface is straightforward. Needless to say, we expect that the fundamental result of this work, that is the enhancement of folding temperature by the attracting interface, will be recovered also in the three dimensional case.

At this point I would like to thank Dr. G.Jug for having suggested this work to me, and for the interest manifested during its progress, and Professor A.Borsellino who, by accepting me in his group, made the conclusion of this work possible.

7.1 Numerical Algorithm for Enumerating Lattice Walks.

The problem of enumerating lattice walks can be split up into two parts. The first consists of generating all the possible configurations, the second in keeping only those which are relevant to us.

Let us consider the walk generation only. In order to have an efficient program, we must first of all generate a given configuration only once, and then generate it in such a way that, if two or more configurations have a common part, this common part will be generated once only. This can be achieved in the following way:

To be as clear as possible, we first consider only the generation of SAWs. We introduce on the lattice cell a labelling of sites as in figure 23.

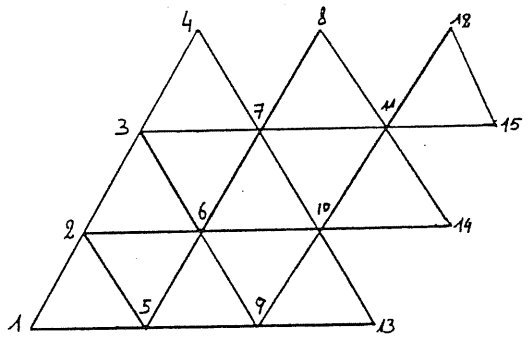

fig.23

We then create an array, let us say a, with as many lines as the number of sites (15 for a 3×3 cell like in figure 23).

To each line we associate a site; for instance, to the fourth line we associate the site number four. All the lines contain six numbers, which are the neighboring sites. If a given site has less than six neighbours, the line will be completed with zeros. For instance, line four will be $(3,7,0,0,0,0)$, while line ten will be $(6,9,13,14,11,7)$. The order of the list of neighbours does not have importance.

We also introduce a vector, let us say c, which contains the current walk. This vector has 27 elements, which is the maximum number of steps in the 3×3 cell. When the program starts, this vector contains only one element different from zero: the first one which contains the value 1. This means that the current site is the origin.

Then the program looks for the last non zero element in the vector c. It finds the value 1, and so goes to the first line in the array a. It then takes the first element of this line, and, putting it in the second place in vector c, considers it like the new current site. We now suppose that this current site is 5.

Then the procedure starts again looking for the last non zero element in the vector c, which is five, so considers line 5, and takes the first element, which becomes the new current site, and so on.

To avoid that the walk returns on an already visited site, we must associate to each site a variable called "occurrence", which contains the value 0 if the site has not yet been visited, and 1 if the site already belongs to the current walk c.

The generation of the first walk goes on until the program encounters an "ending situation", which can be for instance $c = (..., 10, 11, 12, 15, 0, ...)$. Actually, when considering line 15, the program finds that the neighbours of the site 15 are 11, and 12. But both have an occurence 1, and cannot be accepted as new current sites.

When an "ending situation" is encountered, the current walk is analysed; that is to say that we count how many steps are on the surface (n_S), and how many are in the bulk (n_B). We then add one at the (n_B, n_S) element of the configuration array, presented in next appendix.

Then the program takes away the last element of the current vector (15), puts its occurence variable to zero, and again considers the last element of c which is now 12. It then goes to line 12, and considers the next neighbour which is 11. But 11 has occurrence 1, then we are again in an "ending situation" because 11 is also the last element of the list 12. Again we analyse the vector c, and add one to the corresponding element of the configurations array.

Site 12 is then taken away from the current vector, the last element of this vector

(11) is considered to be the current site, and its neighbour list is visited. The program takes the next element in this list (the first one was 12), which can be 8, and we proceed in the way described above, until the first element in vector c, which is 1, is removed. This is the signal of end of the generating procedure.

For generating globular configurations, there are very few fundamental modifications to be introduced. First, the occurrence variable associated with each site must be allowed to take the values $0, 1$, and 2, instead of only 0 and 1. Second, we need a step occurrence variable which can be 0 or 1. In such a way, if we are at site a, before accepting b as a new current site, we check not only the occurrence of site b, which must be less than 2, but also the occurrence of step (a, b), which must be 0.

The generation algorithm just described seems to be very fast, since it can generate about $2 \cdot 10^6$ configurations in less than ten minutes, when written in C language and implemented on a VAX computer.

Unfortunately, at present the program generates some overlapping configurations, which are not physically acceptable. The figure 24a) shows a non overlapping, acceptable configuration, while on figure 24b), we have a "wrong", overlapping configuration.

(a) (b)

fig.24

The procedure eliminating these unphysical configurations is currently under consideration and this is the reason why results for the adsorption of globular and Θ-point phases have not been presented for 3×3 cells.

7.2 SAW and Globule configurations for 2×2 cells.

The elements of the following tables are the coefficients $C^{2\times 2}_{G_m}(n_B, n_S, x = \infty)$ presented in section 3.2. We note that for $m = 0$ we have the SAW configurations.

m = 0

n_B \ n_S	0	1	2
0	0	0	1
1	0	0	1
2	0	3	4
3	2	7	4
4	6	9	0
5	4	4	0
6	0	0	0
7	0	0	0
8	0	0	0
9	0	0	0
10	0	0	0

m = 1

n_B \ n_S	0	1	2
0	0	0	0
1	0	0	0
2	0	0	1
3	0	0	4
4	0	4	6
5	1	13	4
6	5	14	4
7	4	6	0
8	0	0	0
9	0	0	0
10	0	0	0

m = 2

n_B \ n_S	0	1	2
0	0	0	0
1	0	0	0
2	0	0	0
3	0	0	0
4	0	0	2
5	0	0	6
6	0	4	8
7	4	7	6
8	5	5	0
9	0	0	0
10	0	0	0

m = 3

n_B \ n_S	0	1	2
0	0	0	0
1	0	0	0
2	0	0	0
3	0	0	0
4	0	0	0
5	0	0	0
6	0	0	1
7	0	1	1
8	0	1	0
9	0	0	0
10	0	0	0

m = 4

n_B \ n_S	0	1	2
0	0	0	0
1	0	0	0
2	0	0	0
3	0	0	0
4	0	0	0
5	0	0	0
6	0	0	0
7	0	0	1
8	0	0	0
9	0	0	0
10	0	0	0

7.3 SAW configurations for 3×3 cells.

The elements of the following table are the coefficients $C_{G_0}^{3\times 3}(n_B, n_S, x = \infty)$ used in section 5.

m = 0 (SAW)

n_B \ n_S	0	1	2	3
0	0	0	0	1
1	0	0	0	1
2	0	0	4	4
3	0	3	11	14
4	2	18	31	30
5	17	61	81	42
6	59	152	162	44
7	120	268	222	42
8	149	321	222	30
9	109	237	147	12
10	47	98	48	2
11	9	16	6	0
12	0	0	0	0
13	0	0	0	0
14	0	0	0	0
15	0	0	0	0
16	0	0	0	0
17	0	0	0	0
18	0	0	0	0
19	0	0	0	0
20	0	0	0	0
21	0	0	0	0
22	0	0	0	0
23	0	0	0	0
24	0	0	0	0

REFERENCES

[1] P.G. de Gennes: *Scaling Concepts in Polymer Physics* (Cornell Univ. Press, Ithaca 1979).

[2] T.E. Creighton: *Proteins* (W.H. Freemann & Co., 1984).

[3] W. Hoppe, W. Lohmann, H. Markl, H.Ziegler (ed): *Biophysics* (Springer-Verlag, Berlin 1983).

[4] M. Volkenstein: *Biophysique* (Editions MIR, Moscou 1981).

[5] R. Cantor, and P.R. Schimmel: *Biophysical Chemistry* (W.H. Freemann & Co., San Francisco 1980).

[6] H.E. Stanley, P.J. Reynolds, S. Redner, F. Family: *Real Space Renormalisation* (Springer-Verlag, Berlin 1982).

[7] G. Jug, J.Phys.A: Math.Gen**20**, L503(1987).

[8] K. Kremer, J.Phys.A: Math.Gen**16**, 4333(1983).

[9] E. Eisenriegler, K. Kremer, K. Binder, J.Chem.Phys.**77**, 6296(1982).

[10] E. Bouchaud, J. Vannimenus, Preprint(1989).

[11] F. Seno, A.L. Stella, Europhys.Lett.**7**, 605(1988).

[12] P.G. de Gennes, Advances in Colloid and Interface Science **27**, 189(1987).

[13] P.G. de Gennes, J.Phys.**37**, 1445(1976).

[14] B. Albert, D. Bray, J. Lewis, M. Raff, K. Roberts, J. Watson: *Biologia Molecolare della Cellula* (Zanichelli, Bologna 1984).

[15] B.L. Silver: *The Physical Chemistry of Membranes* (Allen & Unwin, London 1985).

[16] F. Jahnig, Springer Ser.Chem.Phys.**11**,344(1980)

[17] C.DeLisi & F.W. Wiegel, Proc.Natl.Acad.Sci.USA**78**, 5569(1981).

[18] S.F. Edwards, Proc.Phys.Soc.**88**, 265(1966).

[19] S.L.A. de Queiroz, C.M. Chaves, Z.Phys.B**40**, 99(1980).

[20] T.W. Burkhardt, E. Eisenriegler, I. Guim, Nucl.Phys.B, (1989).

[21] D.E.Graham and M.C.Phillips, Unilever Research Laboratory (U.K.) Report (1986).